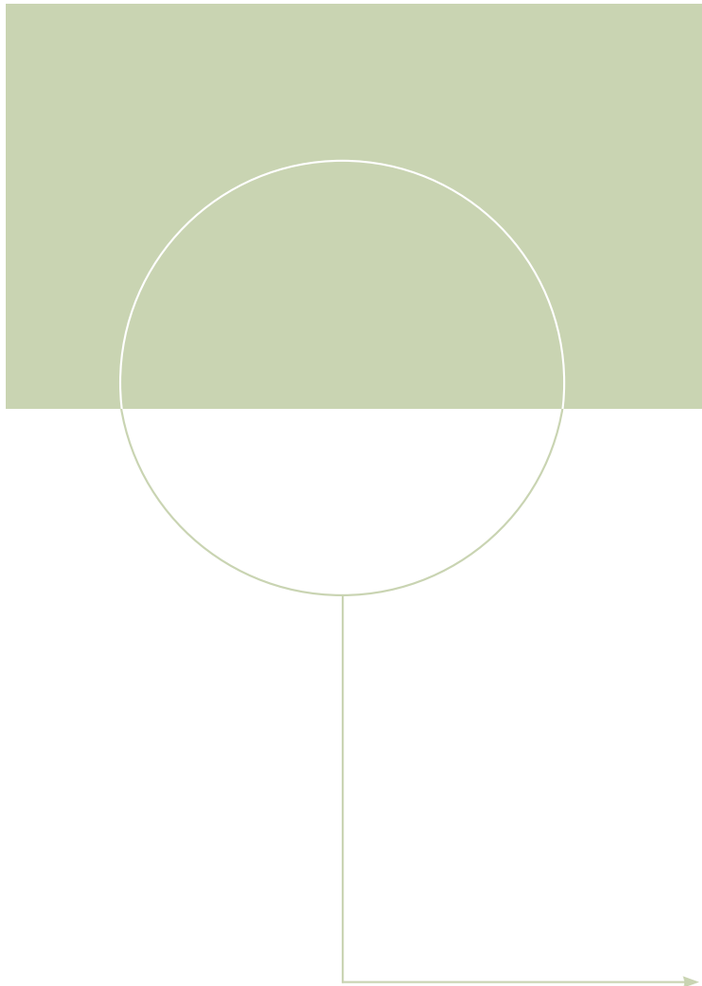

Master's thesis

2019

Kjell Ivar Lian

NTNU
Norwegian University of
Science and Technology
Faculty of Engineering
Department of Marine Technology

Kjell Ivar Lian

Analysis of Riser-induced Loading on Wellhead for Drilling- and Production phase

June 2019

NTNU
Norwegian University of
Science and Technology

NTNU
Norwegian University of
Science and Technology

NTNU

Norwegian University of
Science and Technology

Analysis of Riser-induced Loading on Wellhead for Drilling- and Production phase

Subsea Technology
Submission date: June 2019
Supervisor: Prof. Bernt Johan Leira

Norwegian University of Science and Technology
Department of Marine Technology

NTNU

Scope of work

Master thesis, Spring 2019

for

Stud.Techn. Kjell Ivar Lian

Analysis of Riser-induced loading on Wellhead for drilling- and production phase.

Analyse av stigerørs-indusert belastninger på brønnhode for boring- og produksjonsfasen.

Fatigue of the wellhead for subsea-completed wells is a growing problem. This is partly due to the often extended life of the well from the original plan, due to the drilling of side-wells and the considerable maintenance which is performed, etc. New Blow out Preventers are often larger and heavier and new hydraulic tension systems are applied in order to keep the riser in tension. Especially in shallow water the stress on the wellhead is significant because of the forces transferred from the riser. Cracks in the wellhead can result in leakage and loss of the well. It is therefore of great importance that the load is kept at an acceptable level to ensure the well's integrity. Most of the investigations and studies of wellhead fatigue is considering only the drilling stage of a well, and it is therefore of interest to investigate a larger part of the well`s lifetime and to estimate the damage that the drilling and production stage of a well contribute.

The following subjects are to be examined in this thesis:

1. The candidate shall give a general description of the main components of a drilling and riserless light well intervention system.

2. The candidate shall perform a review of literature related to methods for global analysis of risers and the associated wellhead loading.

3. The candidate shall make himself acquainted with the computer program SIMA/RIFLEX, which is applied for static and dynamic response analysis of marine risers. A brief description of this computer program

and its theoretical basis is also to be given. Describe in detail the differences between the drilling and riserless well intervention systems.

4. Establishing a model of the wellhead, with appurtenant components for local analysis in the analysis program ABAQUS CAE to estimate stress concentrations. Load results from the global analysis in RIFLEX are used. Results from ABAQUS CAE are used in the fatigue assessments to evaluate the safety margin in relation to the fatigue capacity. A brief summary of the program and the theoretical basis it is based on is presented.

5. Parameter variation for variables that is important with respect to the fatigue life of the wellhead. A relevant issue will be the applied top tension and possible currents in the environment

In the thesis the candidate shall present his personal contribution to the resolution of problems within the scope of the thesis work. Theories and conclusions should be based on mathematical derivations and/or logic reasoning identifying the various steps in the deduction. The candidate should utilise the existing possibilities for obtaining relevant literature.

The thesis should be organised in a rational manner to give a clear exposition of results, assessments, and conclusions. The text should be brief and to the point, with a clear language. Telegraphic language
should be avoided.

The thesis shall contain the following elements: A text defining the scope, preface, list of contents,
summary, main body of thesis, conclusions with recommendations for further work, list of symbols and
acronyms, references and (optional) appendices. All figures, tables and equations shall be numerated.

The supervisor may require that the candidate, at an early stage of the work, presents a written plan for the completion of the work.

The original contribution of the candidate and material taken from other sources shall be clearly defined.
Work from other sources shall be properly referenced using an acknowledged referencing system.

NTNU

The thesis shall be submitted in 3 copies:

- Signed by the candidate
- The text defining the scope included
- In bound volume(s)
- Drawing and/or computer prints which cannot be bound should be organised in a separate folder

Supervisor: Professor Bernt J. Leira
Deadline: June 11th 2019

Trondheim, January 15th, 2019

Bernt J. Leira

Preface

This report is a result of my Master of Science thesis, which is written in my last semester in the two year Master's degree program within Subsea Technology at the department of Marine Technology at the Norwegian University of Science and Technology. The thesis is follow-up and a further development of the project carried out in the fall of 2018 where relevant computer programs and theory for riser- and wellhead fatigue analysis were studied.

I would like to thank Sigbjørn Sangesland and my supervisor Professor Bernt J. Leira for presenting the project thesis and for the guidance during the project- and master periods. The necessary data, guidance and discussions they have provided and participated in have been essential for the completion of this thesis.

Trondheim, 7th of June, 2019

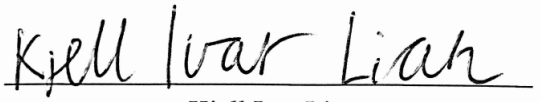

Kjell Ivar Lian

Summary

Fatigue of wellhead at subsea-completed wells is a growing problem in the offshore industry. Large forces are transmitted from the marine riser system and down to the wellhead that causes fatigue, and the lifetime of a well is increasing as a result of technology development. The development of new technology like RLWI has also increased the number of interventions, and the number a well can experience may vary from well to well. Most studies and investigation of wellhead fatigue only consider the drilling stage of a well. As a consequence, the production and decommissioning stage of the well is omitted in the calculations. It is therefore of interest to investigate a greater part of the well‘s lifetime, and to estimate the damage that the drilling- and production stage of a well contributes with.

The thesis can be divided into two parts. The first part is a literature study where relevant theory is presented. This includes a description of the drilling stage, information about RLWI and its main components and fatigue analysis. An introduction to the software RIFLEX and ABAQUS will then be presented. A local model of a wellhead is created in ABAQUS to quantify stress concentration factors, while RIFLEX is used for the global analysis and post processing. The second part of the thesis presents the two different global models. One of the models represents a RLWI stack with a 9” riser, the second model is representing a drilling riser system provided by MARINTEK. This presentation shows more thoroughly the differences between an intervention operation using a RLWI- and a drilling riser system. Results from the local analysis in ABAQUS and the post-processed results in RIFLEX are presented in the result section of the thesis.

Investigation of fatigue damage due to the drilling phase and interventions has been conducted. The obtained results has shown that an intervention contributes with minimal damage. Even with several intervention operations, the damage is close to insignificant. The wellhead fatigue assessment has proven to be sufficient during the two first stages to the well, the drilling- and production stage. It is therefore, in view of the remaining fatigue life of the well, likely that the well will be able to withstand the forces from of the final stage, decommissioning.
The results from the parameter studies where current and top tension were used as variables gave similar results, the intervention operations contributes with minimal damage. However, variable top tension influence the two systems differently. It is observed that the RLWI system is negatively influenced by a higher top tension, while the drilling system benefits from it. This shows that the RLWI system transfer less forces with a more flexible system, while the drilling

riser transfer less forces with a stiffer system. Both systems benefits from a current in the environment. The results has proven that the effect of current is greater for the drilling riser than for the RLWI riser. This is believed to be the effect of a larger hydrodynamic damping that comes with larger cross-sections.

Sammendrag

Utmatting av undervanns brønnhoder er et voksende problem i offshore industrien. Store krefter blir overført fra stigerørssytemet og ned til brønnhodet som forårsaker utmatting, og levetiden til en brønn øker som et resultat av teknologiutvikling. Utviklingen av ny teknologi som RLWI systemet har også økt antallet intervensjoner, og antallet kan variere fra brønn til brønn. De fleste studier og undersøkelser av utmatting i brønnhodet ser bare på borefasen til brønnen. Konsekvensen av det er at produksjons- og nedleggelsesfasen til brønnen blir utelatt i beregningene. Det er derfor interessant å undersøke en større del av brønnens levetid og å estimere skaden som bore- og produksjonsfasen til brønnen bidrar til.

Oppgaven kan bli delt inn i to deler. Den første delen er en litteraturstudie hvor relevant teori blir presentert. Dette inkluderer en beskrivelse av borefasen, information om RLWI og dets hovedkomponenter og teori om utmatting. En introduksjon av programvarene RIFLEX og ABAQUS vil deretter bli presentert. En lokal modell av brønnhodet er laget i ABAQUS for å angi størrelsen av stress konsentrasjoner, mens RIFLEX brukes til global analyse og etterbehandling. Den andre delen av oppgaven presenterer to forskjellige globale modeller. Den ene globale modellen representerer et RLWI system med et 9” stigerør, den andre modellen representert et borestigerørsystem gitt av MARINTEK. Denne presentasjonen viser mer grundig forskjellene mellom en operasjon i form av intervensjoon ved bruk av RLWI og et borestigerørsystem. Resultatene fra den lokale analysen i ABAQUS og de etterbehandlende resultatene i RIFLEX er presentert i kapittelet som omhandler resultat.

Undersøkelser av utmattelsesskader under borefasen og intervensjoner har blitt gjennomført. De oppnådde resultatene har vist at en intervensjon bidrar med minimal skade. Selv med flere intervensjonsoperasjoner er skaden nesten ubetydelig. Utmattelsesvurderingene av brønnhodet har vist at det er tilstrekkelig kapasitet for de to første fasene til en brønn, bore- og produksjonsfasen. Der er derfor, med hensyn til det resterende levetiden til brønnen, sannsynlig at brønnen vil være i stand til stå mot kreftene fra den siste fasen, avviklingsfasen. Resultatene fra parameterstudiene hvor strømninger og toppspenninger har blitt brukt som variabler har gitt lignende resultater, intervensjon operasjoner bidrar med minimal skade. Toppspenningen påvirker imidlertid de to systemene forskjellig. Det er obersevert at RLWI systemet er negativt påvirket av en høy toppspenning, mens stigerøret til boresystemet drar nytte av det. Dette viser at RLWI systemet overfører mindre krefter ved et mer fleksibelt system mens

boresystemet overfører mindre krefter med et stivere system. Begge systemene drar nytte av at det er strøm i miljøet. Resultatene har vist at effekten av strøm er større for stigerørssytemet til boresystemet enn for RLWI stigerøret. Det antas at dette kommer av en større hydrodynamisk demping ved bruk av større tverrsnitt.

Table of Contents

List of Tables

List of Figures

Nomenclature

Abbreviations

API American Petroleum Institute
BOP Blowout Preventer
DNV Det Norske Veritas
JONSWAP Joint North Sea Wave Observation Project
LMRP Lower Marine Riser Package
MODU Mobile Offshore Drilling Unit
ID Inner diameter
OD Outer diameter
WH Wellhead
XT Christmas tree
EA Axial stiffness
EI Bending stiffness
WCP Well control package
LLP Lower lubricator package
PCH Pressure control head
LUB Lubrication tubular
IMR Inspection, maintenance and repair
DSB Dual stuffing box
USB Upper stuffing box
MEG Methanol and glycol injection
SCM Subsea control module
eSCM Electric subsea control module
UTH Umbilical Termination Head
PM Pierson-Moscowitz
SCF Stress concentration factor
DFF Design fatigue factor
IMR Inspection, maintenance and repair
IMO Wellhead
WH International Maritime Organization

CT Coiled Tubing
DAF Dynamic Amplification Factor

Chapter 1

Introduction

Fatigue loading on subsea wellhead is a problem that has been around for a time and is a concern that is only becoming more present. Some of the reasons can be e.g the increase of size and weight of the blow out preventer, the riser is constantly kept under tension from a hydraulic system resulting in high forces at the wellhead and so on. Another reason is the extension of lifetime for a well, new side-wells and maintenance of the wells is increasing the overall lifetime for what was first intended. This can obviously bring problems considering fatigue life for the wellhead. Fatigue damage on wellhead due to high stresses is especially a problem in shallow water, where large forces from the riser is transferred to the wellhead.

New technology for well intervention have been introduced for several reasons. One reason is the safety considering fatigue, trying to avoid potential disasters. Another reason is the cost saving opportunities. Riserless well intervention(RWLI) is a newer technique that has been developed in the later decades. Well interventions can be performed at a much lower cost while at the same time gives the opportunity to increase the oil recovery rate.

The scope of this thesis is to conduct a literature study of relevant theory and to build a global model of a RLWI system with relevant components. Dynamic analysis of the RLWI system and an example provided by MARINTEK of a standard operation should be performed. The results from the two different systems might show the possible benefits using a lighter system rather than a heavier one. In addition, a local analysis of a wellhead should be conducted to estimate potential stress concentration factors that a global analysis is not capable to detect.

The literature study presents several themes, starting with a description of a drilling riser system. Relevant literature for a RLWI system with components will be presented. Information about fatigue analysis will also be described as well as environmental forces. The last part of the thesis specifies the local and global models, results, conclusion and further work.

1.0.1 Organization of Thesis

Chapter 2 - Description of the two different systems and environmental loads.
Chapter 3 - Relevant fatigue theory .
Chapter 4 - Riser analysis and theory.
Chapter 5 - Theory and information for the RIFLEX software and information about the global models.
Chapter 6 - Description of local model and theory for the ABAQUS software.
Chapter 7 - Procedures and simulations for the thesis.
Chapter 8 - Presentation of the results and a discussion of the results from the local and global fatigue calculations.
Chapter 9 - Conclusion to summarize the results and the consequences they have.

The literature and theory chapters are to a high extent information obtained from the project thesis (Lian (2018)).

Chapter 2

System Description

The process of drilling a well and extract oil and gas from the hydrocarbon reservoir is a complex operation having a long duration. It is possible to divide the process into four phases, exploration, drilling, production and when the well gets dry after production, plugging and abandonment. It is usual to perform seismic survey for mapping of the soil before drilling. If the survey is positive, a exploration/wildcat test well is drilled to investigate if the reservoir actually contain hydrocarbons. Casings are set in place if the wildcat was positive, and after the commissioning the production can start (Mather (2011)).

2.1 Drilling Facilities

There are several different drilling units from fixed platforms to mobile offshore drilling units (MODU). Within the MODU types, there are primary three different rig types, drill ship, jack-up and semi-submersible. The rig controls and supports the entire drilling operation and is the connection point above the sea level for the marine riser and drill string. For the choice of drilling unit, several requirements must be taken into account. Cost, deck area and environmental condition are all important factors, but water depth is the most important factor for choice (Maclachlan (1987)). Figure 2.1 shows an overview of different drilling units over varying water depth.

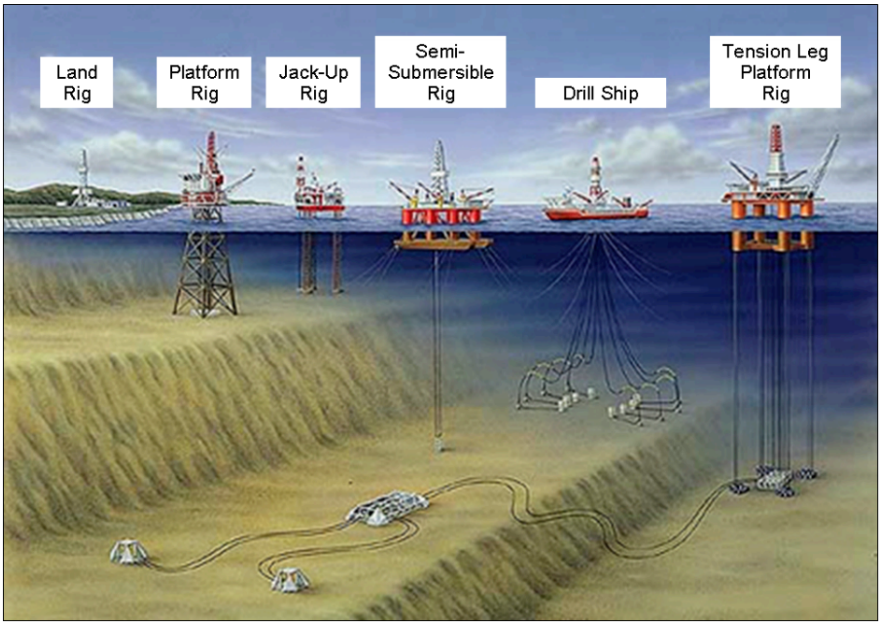

Figure 2.1: Overview of drilling rigs over varying water depths.

Relative motions of the marine riser will depend on the rig type. Except the environmental loads, the floaters will have a vessel motions resulting in additional load on the riser. The additional force can cause the fatigue life of the system to be lowered.

2.2 Drilling a Well

The drilling process may vary from well to well due to bottom condition, water depths, information about the reservoir from seismic survey and so on. For any well, there are still three main steps. Drilling, completion and workover (DNVGL-RP-0142 (2015)). This section will give a general description of the drilling stage and is to a high extent based on Sangesland compendium, *Introduction to drilling and completion of subsea wells*.

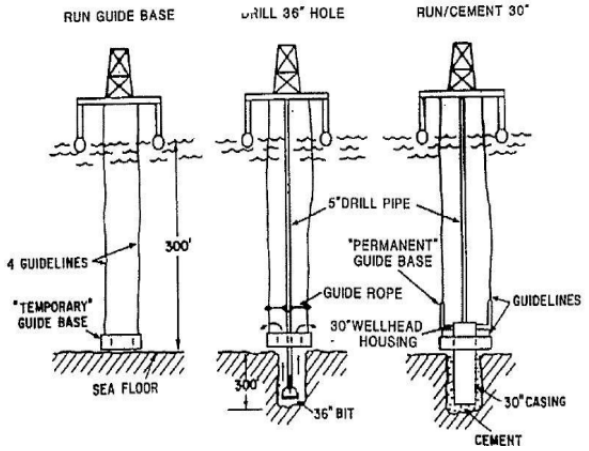

Figure 2.2: Illustration of the three first steps for drilling a well.

The first step in figure 2.2 shows the installment of the temporary guide base. The following bullet points describe the installment phase and the drilling stage after the temporary guide base is in place.

- The purpose with the guide base is to verify that the equipment is placed in the right position on the seabed.
- After the temporary guide base is installed, a 36” drill bit drills the first part before installing a 30” casing. Every area between the drill hole and casing will be cemented and secured before proceeding.
- Before drilling with a 26” bit and installing 20” casing, the formation around the conductor needs time to obtain sufficient skin friction between the formation and conductor. This takes usually between two to four hours.
- Next, the wellhead is attached on the top of 20” casing and inside the conductor.

- Now, the blow out preventer (BOP) and marine drilling riser are run and connected to the wellhead. The drilling continues afterwards.
- First with a bit size 17.5” and corresponding casing 13 3/8”. A 12 1/4” bit drills the 9 5/8” casing before finally a 8 1/2” bit is used to drill the hole section for the 7” liner.

Figure 2.3 and table 2.1 shows the last three steps for drilling operation of a well and barriers during drilling of different sections, respectively.

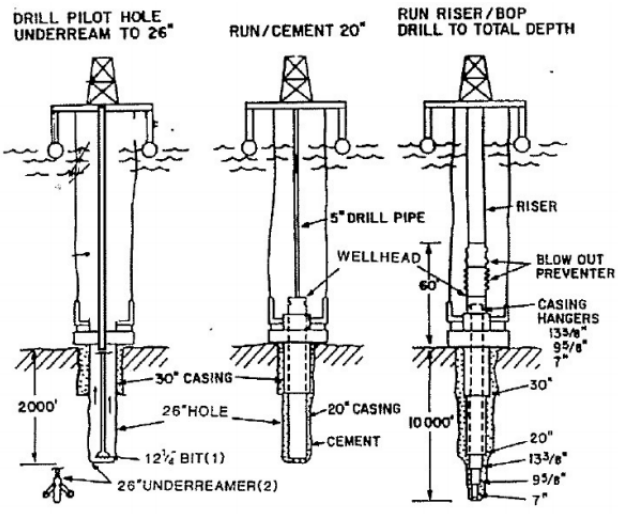

Figure 2.3: Illustration of the three last steps for drilling a well.

Hole size (inch)	Casing Size (inch)	Typical depth below seabed (m)	Type of drl. fluids	Drlg. Riser & diverter installed	Press. barrier no. 1	Press. barrier no. 2
36	30	80	Seawater (1)	No	-	-
26	20	500	Seawater (1)	No	-	-
17 ½	13 3/8	2000	Mud	Yes	Mud	BOP
12 ¼	9 5/8	3000	Mud	Yes	Mud	BOP
8 1/2	7 liner	4000	Mud	Yes	Mud	BOP

Table 2.1: Common pressure barriers (Sangesland (2016).

2.3 Wellhead

The wellhead is located at the seabed and installed inside the conductor housing. Inside the wellhead, the tubing head and casing heads are located. It is common that during drilling that the BOP is fastened to the wellhead, while during production an X-mas tree is placed at the top of the wellhead. It is also possible to mount the BOP directly onto a X-mas tree. Then the tree will be between the wellhead and the BOP. The wellhead provides a safety barrier to avoid fluids to penetrate the surroundings after it is installed. The subsea wellhead will usually consist of drilling guide base, low-pressure housing, high-pressure housing, bore protectors and wear brushings casing hangars, running and test tools, metal to metal annulus sealing assembly and casing hangars (Petrowiki (2018)).

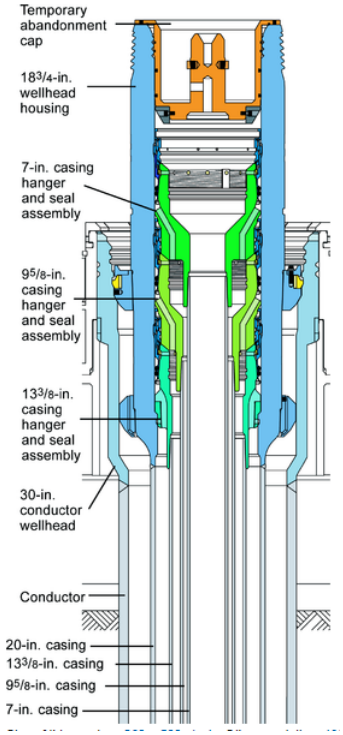

Figure 2.4: Illustration of wellhead system (Petrowiki (2018)).

2.4 Blowout Preventer

The blowout preventer stack consists of well control equipment including the BOP itself, spools, valves, hydraulic connectors, and nipples to connect the BOP to the wellhead. The main purpose of the BOP is to ensure pressure control in the well while a drilling riser is connected to it. If the well gets unstable and uncontrollable, the BOP can close the well immediately to enter a safe condition. The BOP stack can be divided into two parts, the BOP and the lower marine riser package(LMRP), respectively. The BOP is placed directly on the wellhead with the LMRP placed on top. This makes it possible to to disconnect the LMRP from the BOP during an emergency or any other reasons. It is necessary for analyses of the marine to be aware that the BOP is very rigid compared to the marine riser. Hence, the marine riser system will be rigid between the wellhead and the marine riser (Bai and Bai (2005)).

2.5 Well Intervention

At some time point in the life span from the start of production to the abandonment, there will be a need for maintenance of the well. This can for example be sensors that fails, formation pressure declines, moving parts and seals wear out (Flatern (2016)). Well intervention can be divided into three different categories, light, medium and heavy intervention. In Figure 2.5 light, medium and heavy are categorized as A, B and C, respectively. Heavy intervention, also referred to as workover, is often used to pull tubing string or redrill the well. This intervention method requires drilling rig to run marine riser and BOP to contain pressure from the well bore.

Light well interventions can be performed in existing X-mas trees by using either wireline or coiled tubing (Paaske (2017)). Light well intervention can execute operations like clear the well of sand, paraffin, hydrates or other material that affects the performance of the well. Medium intervention can compared to light intervention perform operations with more complex intervention tools due to larger deck space, and usually attach rigid risers in deeper water.

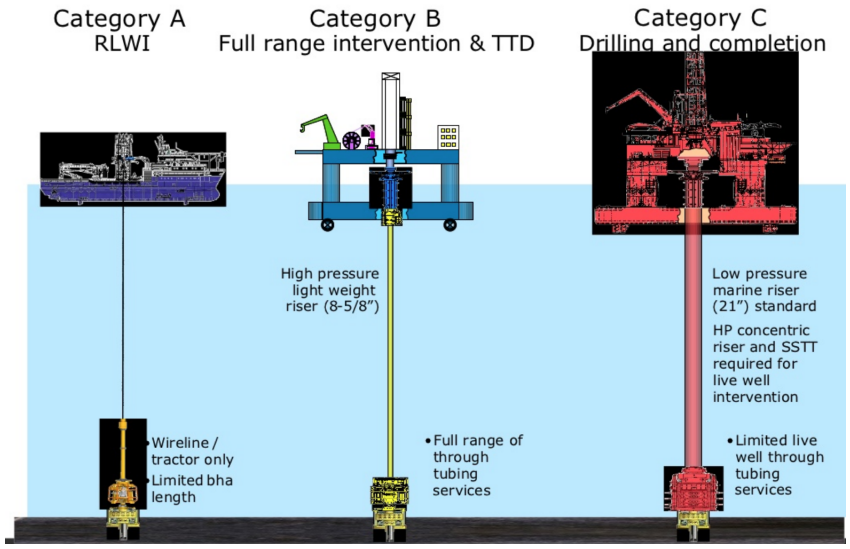

Figure 2.5: Categories of well intervention (Jensen (2008)).

Category A representing RLWI can be further subdivided into subcategories. Except the traditional Category A, Category A+ and Category A++ can be considered as RLWI operations. It is possible to separated between the three sub categories as follows:

- **Cateogry A** - Using wireline and typically a monohull due to capital cost and cost of transit.
- **Cateogry A+** - Wireline and coiled tubing, also typically using a monohull vessel. Coiled tubing offer a greater capability, but it is not able to work full bore 7-9” which restricts what can be done.
- **Cateogry A++** - Wireline and coiled tubing deployed via a 7-9” riser. Has the benefit of the ability to full bore with coiled tubing through 7” bore of the well. The overall cost is increasing with this method, which is a disadvantage.

2.6 Riserless Light Well Intervention

Riserless ligth well intervention(RLWI) has the ability to perform interventions by using wireline or a smaller risers like 7-9" instead of a 21" riser. Because of the size of the vessel used for e.g workovers using a 21" riser, the cost of an intervention is high and time demanding, causing the operator from not intervening the well. According to Friedberg et al. (2010), platform wells will be maintenance at least every fourth year, while subsea wells is less frequent. As a result the platform wells will have a larger recovery rate compared to the subsea wells. Using wireline intervention provides an opportunity to the operator to perform well intervention regularly and in an economical way by using a monohull vessel.

2.7 Main system for RLWI

2.7.1 Vessel

The vessel is designed to have sufficient place for intervention tools, and the main components onboard are heave compensation system, skidding system, moonpool, crane system and dynamic positioning system. Different operations require different equipment. For example, an operation for a dead well require different equipment than an operation of a live well (Harestad (2018)). Rules and regulations require the vessel in RLWI operations to satisfy Dynamic Positioning Class 3.

2.7.2 Positioning

Controlling the position of the vessel during operation is important to avoid drift off, pollution damage and other serious accidents. This applies to the environment as well as the financial consequences for the companies. Beyond the safety aspect, the dynamic positioning (DP) system is important to gain accuracy when lowering the equipment to the seabed. The dynamic positioning system on the vessel use Global Positioning System (GPS). The GPS uses sensors for wind and waves, and also gyro compasses to calculate the vessels position, magnitude and the environmental forces. The vessels thrusters and propellers automatically maintain the wanted position for the vessel based on the gathered information. As mentioned, the vessel needs to satisfy the international maritime organization(IMO) class 3 for dynamic positioning. The regulations requires class three if: *Operations where loss of position keeping capability may cause fatal accidents, or severe pollution or damage with major economic consequences* (DNVGL-RP-E307 (2015)).

2.7.3 Moonpool

Moonpools are openings located in the hull of the vessel providing access to deploy and retrieve equipment from the sea without operating on the side of the vessel. With a moonpool the operation window becomes greater i.e can operate in harsher environment. The moonpool is often placed close to the vessels roll and pitch center, thus reducing the motions on equipment being lowered and retrieved.

2.7.4 Module Handling Tower (MHT)

The module handling tower is a structure made of steel beams and is commonly used to handle equipment for inspection, maintenance and repair (IMR) services. It is supported by four legs on the main deck, and two cursors systems are installed for safety reasons and to have the ability to deploy and retrieve equipment. While the upper cursor is used to hook up the tools during lifting into the moonpool, the lower cursors are used to restrain sideways movement of the equipment from the tower down to the vessels keel (Axtech (2018)).

2.7.5 Heave Compensator

During any offshore operation, the vessel will encounter wave forces that makes the vessel move up and down due to heave motion. The heave compensation system purpose is to minimize the relative velocity between the vessel and the equipment being lowered. Usually the crane, wireline system and the umbilical will have installed heave compensators. The wireline compensator is installed at the upper wireline sheave wheel located in the module handling tower. The umbilical compensation system will normally consist of two fixed sheaves and one compensation sheave(Mathiassen et al. (2008)).

2.7.6 RLWI Stack

Figure 2.6 shows the FMC Technologies RLWI Stack #4 and the different components in the stack. The stack can be divided into two parts, lower and upper. The upper part includes the PCH, ULP and LLP. The lower part consists of the WCP.

This subsection will provide information of how a RLWI system can be built. Companies and manufactures have different solutions for the system. Hence, this information is therefore just an example and not an answer to how the an RLWI system must be built. For example, the subsea control module(SCM) can be placed in the WCP from one manufacturer, while from a competitor the SCM can

be placed in the LLP. However, the functionality and user interface for the different RLWI systems are basically the same. Information about the different components is retrieved from Birkeland (2005).

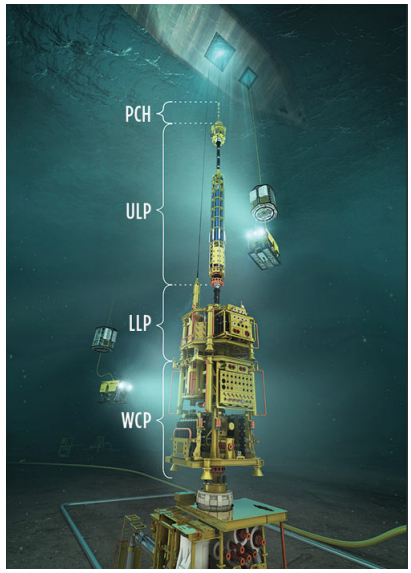

Figure 2.6: Main components of RLWI #4 (FMC Technologies(2015).

- **Pressure Control Head(PCH)**
  This component is located on top of the RLWI lubricator and provides a pressure barrier and seal during wireline operations. It contains grease to lubricate and to create a seal around the moving wireline. The pressure from the grease should be higher than the well pressure for safety reasons, because a higher pressure will avoid oil and gas to flow out of the well. The PCH contains the upper and dual stuffing boxes. These creates in total two sealing elements. Upper stuffing box(USB) works as a static seal on a stationary wireline. The dual stuffing box(DSB) is located between the tool catcher and the flow tubes. It is supplied with a grease injection point between every rubber element and works as a back-up element. During an operation, viscous grease is injected in the flow tubes to make the pressure rise inside the PCH until it is higher than the well pressure.

  The dual stuffing box is located, as mentioned, between the flow tubes and the tool catcher, and it is equipped with a grease injection point between each rubber element working as a back-up barrier element. The main

purpose is to seal fluid or gas pressures to the wellbore. During operations, the DSB also works as a grease injector and has connection point for hoses. DSB has the function for MEG injection, although it is not normally used for this purpose.

- **Upper Lubricator Package(ULP) and Lubricator Tubular(LUB)**
  The ULP is the connection between the Pressure Control Head and the Lubrication Tubular. Figure 2.6 is only mentioning the ULP with name and not the LUB. This is because the LUB is integrated in the ULP in this stack. The ULP is installed with a Cutting Ball Valve and has the capability to shear off 7/16" braided cable and up to 7" lubricator diameter if there is an emergency. It has two mono-ethylene glycol(MEG) injection points for hydrate prevention. The lubrication tubular contains grease reservoirs and high-pressure injection pumps. These grease reservoirs work as storage for the grease to maintain the well pressure. Also, the LUB can hold the tool string prior to entering the well. First, the tool string is kept inside the LUB. Second, the LUB is sealed off and the pressure is increasing until it reaches the well pressure. After the system is pressurized the stool string can safely be lowered into the well.

- **LLP**
  The Lower Lubrication Package is placed between ULP and the Well Control Package and connects these two together. The LLP consist of a well kill hub and grease injection system for the wireline, and it carries the main control system for the WCP. Control modules, power supply, hydraulic power and accumulators for the WCP, X-mas tree and PCH are located in the LLP. The lower LLP has a safety join to prevent overload of the X-mas tree and the wellhead.

- **WCP**
  The Well Control Package is placed on top off the X-mas tree and forms the main well safety barrier during intervention. It has the same purpose as BOP during drilling, and it is compatible with both horizontal and vertical X-mas trees. As for the BOP, the WCP has shear seal ram able to cut the wireline, coiled tubing or wireline tool string. It consists of an upper valve block and a lower valve block. The WCP enables the hydrocarbon the flush back into the well and provide hydraulic energy to operate the WCP and the subsea tree valves, while at the same time control and communicate with

the subsea tree functions. Main components of the WCP can be Subsea Control Module(SCM), Umbilical Termination Head(UTH), Well kill hub, Electric Subsea Control Module(eSCM).

2.7.7 Wireline

There a several different categories for wirelines, but the most common ones are braided wire, slickline and power/composite cable. Wirelines are used by attaching tools at the end of the cable or wire before lowering it to the well through a stuffing box. This can be done either with diesel, electro-hydraulic or fully electric driven winch. The three different types of wireline categories, slickline, braided wire and power/composite cable will be presented in the following.

- Slickline (S-Line)
  Consists of only a solid wireline and is used to perform mechanical work. This line is possible to use for several kinds of operations since it is possible to attach different types of tools and equipment. Examples of operations may be pulling tools, running tools, wireline finder, bailer. Typical dimensions for slickline can range from 3/32”, 7/64”, and 1/8” in diameter (Khurana et al. (2003)).

- Braided Line
  There are two types of braided lines, one with electric cable and one without electric cable. The one without electric cable is used for heavier fishing operations(retrieving dropped equipment or tools). Braided line with electric cable can transmit data to the surface logging task and tractor operations. The most common size for braided lines is 3/16”, though for heavier applications 1/4” and 5/16” can be used. For the larger sizes it might be necessary to kill the well due to the wellhead pressure on the relatively large cross-section area on the line (Schlumberger (2018)).

- Composite/Electric Line
  The composite wireline is capable to perform all light intervention operation in subsea wells. This cable has higher strength, lighter weight and can transport more electrical power compared to previous described wireline solutions. Figure 2.7 shows the cross section of a composite cable, consisting of three insulated copper conductors surrounded by carbon fibre in a matrix of thermosetting plastic. This composite cable can handle

higher temperature and pressure during operations compared with braided and S-line.

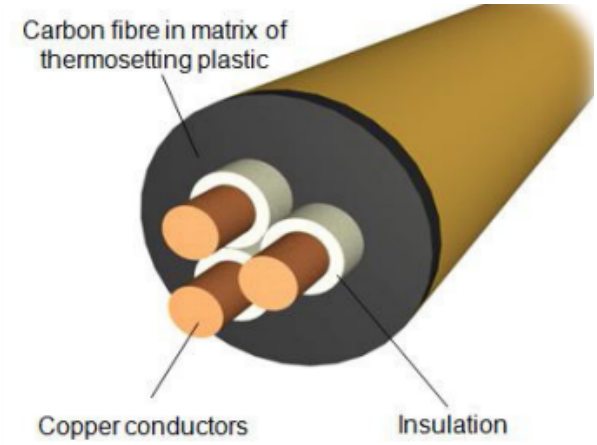

Figure 2.7: Illustration of composite cable (Lindland et al. (2003)).

Table 2.2 shows typical tasks and what kinds of operations the different lines are capable of performing.

Slick line	Braided line	Electrical line
• Running and pulling plugs, chokes, valves. • Opening and closing circulation devices. • Running gas lift or chemical injection equipment.	• Heavier and deeper work outside the working scope of slick line. • Fishing for larger lost objects. • Pulling and retrieving WL-SCSSV.	• Data gathering/ logging tools. • Perforation. • Chemical cutting • Setting packers and bridge plugs. • Determining freepoint (stuckpoint)

Table 2.2: Typical tasks for Wireline operations.

2.8 Coiled Tubing

Coiled tubing (CT) is a welded tube with a relatively small diameter. Standard dimensions for CT is 3/4- to $3^1/_2$ in outer diameter. The tube is welded together by using high-frequency induction without addition filler metal. After the tube is welded, it is dressed off smooth, cleaned and, finally, x-ray inspection is executed to ensure the that the weld is free from defects. The tube is then reeled around a large drum for storage, transport and deployment. CT was developed to work in live wellbores, but CT has proven to be useful in other ways also. Some of the key benefits with CT technology are as follows:

- Ability to work on live wells without shutting down the well,
- Safe and efficient well intervention,
- Less need for crew/personnel,
- Fast mobilization.

The advantage with CT compared with wireline operations is the possibility to circulate fluids to the well. The coiled tube has higher strength than wireline, and can carry the weight of longer and heavier equipment. CT can also be used in wells which has a long, horizontal and complicated traction. The CT can also be applied in the following operations; installation of completion equipment, fishing operations, conveying well logging tools, cleanout and removal of fill materials that restrict flow through tubing or casing, etc.

2.9 Environmental Loads

During marine operations, a structure in the environment will experience waves, currents and wind. They contribute with the so-called environmental forces, and are the main contributors to dynamic loading. To be able to perform an offshore operation in a safe manner, it is crucial to quantify the magnitude of these forces. The following will give an introduction to how the environmental loads can be considered and described in an analysis.

2.9.1 Hydrodynamic Loads

Calculating forces from waves and currents for a riser is specified in DNV's rules and regulations. The standard uses Morison's equation with horizontal movement to provide the most accurate results. Equation 2.1 is retrieved and explained from DNV-OS-F201 (2010).

$$dF = \frac{1}{2}\rho C_D D_H |u - \dot{x}|(u - \dot{x}) + \rho \frac{\pi D_B^2}{4} C_M a - \rho \frac{\pi D_b^2}{4}(C_M - 1)\ddot{x} \qquad (2.1)$$

where
dF Force per unit length
C_M, C_D Inertia and Drag coefficients
D_B, D_H Buyancy-and Hydrodynamic parameter
$\dot{x}, \ddot{x}$, Velocity- and Acceleration of structure
ρ Water denisty
u, a Velocity- and Acceleration of water particle
The last term of Morisons equation includes the added mass $(C_A = C_M - 1)$, which is included in the mass matrix. This term affects the eigenmodes and eigenperiods of the riser.

When regular waves and deep water is assumed, the wave potential can be written as (Pettersen (2007)):

$$\phi = \frac{g\zeta_A}{\omega} e^{kz} sin(kx - \omega t) \qquad (2.2)$$

where k is the wave number $\omega^2 = kg$, while ζ_A is the wave amplitude. The particle speed(u) and acceleration(a) are calculated as:

$$u = \frac{\partial \phi}{\partial x} \qquad a = \frac{\partial u}{\partial t} \qquad (2.3)$$

Inserting this in Morison's Equation 2.1, the drag force varies with sin x|sin x|, while the inertia force varies with cos x. Figure 2.8 shows the drag and inertia force with time as variable.

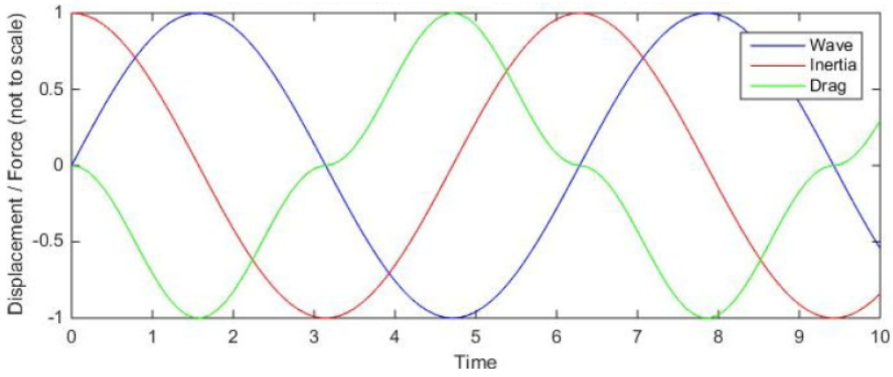

Figure 2.8: Variation of Inertia and Drag force for a regular wave.

The figure shows that the inertia and drag force have a phase difference, and the maximum values occurs at different times.

Currents can be assumed to be constant in an analysis. Hence, there will be no dynamic loading from cur,rent and the current can be assumed to be static. According to Larsen (1990), the force from currents can be calculated as:

$$F_D^{Static} = \frac{1}{2}\rho C_D u_c |u_c| \tag{2.4}$$

where u_c is the current velocity, ρ is water density and C_D is the drag coefficient. If a dynamic analysis is based on the result of the static analysis, the static load is "remembered" by the system. Normally only dynamic loads are included in the dynamic analyses, but the current velocity is quadratic in the drag term of Morison's equation. Because of the values from the static forces this term needs to be included in the dynamic analysis. The force in a dynamic analysis should according to Larsen (1990), be based on Morison's equation, where F_D is the total drag force.

$$F_D^{Dynamic} = F_D - F_D^{Static} \tag{2.5}$$

2.9.2 Wave Spectrum

The frequency decomposition of the sea state is represented by a wave spectrum, $S(\omega)$. The spectrum and the wave amplitude can expressed as (Pettersen (2007)):

$$\frac{1}{2}\zeta_{an}^2 = S(\omega_n)\Delta\omega \tag{2.6}$$

Rewriting the equation with respect to ζ_{an}:

$$\zeta_{an} = \sqrt{2S(\omega_n)\Delta\omega} \tag{2.7}$$

where $\Delta\omega$ is the increment over the frequency interval in the wave spectrum.

The wave spectrum, $S(\omega)$, needs to match a curve. JONSWAP and Pierson-Moscowitz(PM) spectra are the most commonly used and recommended. Pierson-Moscowitz has been established through measurements in the North Atlantic, and it is based on the theory that if winds blows steadily for a long time over a vast area, the waves will come into equilibrium with the wind. Hence, the spectrum characterize an entirely developed sea. From DNVGL-RP-H103 (2011), the Pierson-Moscowitz spectrum is defined as:

$$S_{PM}(\omega) = \frac{5}{16}H_s^2\omega_p^4\omega^{-5}exp\left(-\frac{5}{4}\left(\frac{\omega}{\omega_P}\right)^{-4}\right) \tag{2.8}$$

where ω_p is the peak wave frequency, while H_s is the significant wave height. The main difference between the JONSWAP and Pierson-Moscowitz is that JONSWAP is never fully developed. Instead it is assumed that the sea continues to develop non-linearly through wave to wave interactions for a long period of time and distance. In the rules and regulations given by DNV, the JONSWAP spectrum can be written as:

$$S_J(\omega) = A_\gamma S_{PM}(\omega)\gamma^{exp}\left(-0.5\left(\frac{\omega-\omega_p}{\sigma\omega_p}\right)^2\right) \tag{2.9}$$

Figure 2.9 shows the difference between JONSWAP and Pierson-Moscowitz spectrum. While JONSWAP is referred to as narrow-banded, the Pierson-Moscowitz spectrum is referred to as broad-banded.

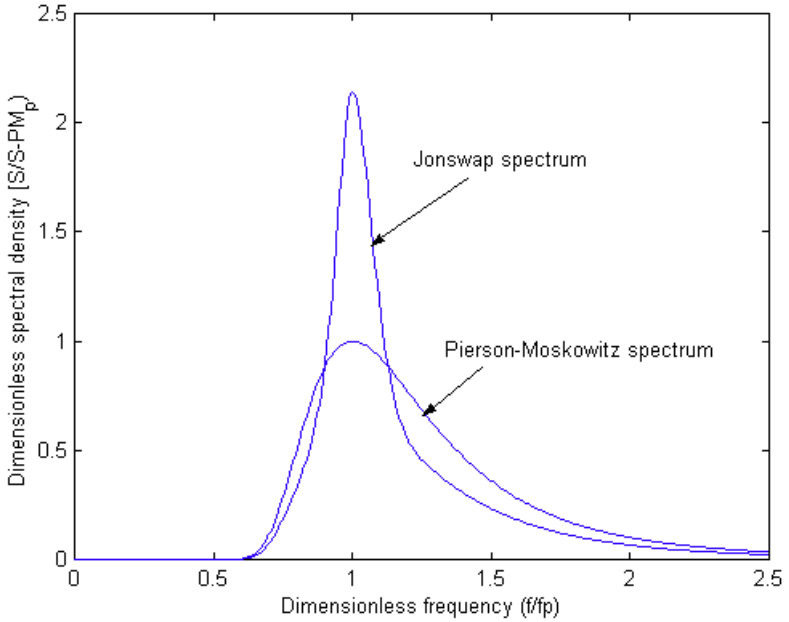

Figure 2.9: JONSWAP and Pierson-Moscowitz spectra.

2.9.3 Effective Tension

The effective tension can be described as the force in a pipe that affects the stability, and is the axial wall force adjusted for contributions from external and internal pressure. This force is relevant for governing the shape of cables and pipes including buckling analysis, and is used for calculation of geometric stiffness in the finite element method. With a negative effective tension, the drilling riser might buckle. The effective tension can be calculated as:

$$T = T_P + A_e P_e - A_i P_i - \rho_i A_i v_i^2 \tag{2.10}$$

where T is effective tension, T_p is tension in pipe wall, $A_{e,i}$ is external/internal cross sectionals and $P_{e,i}$ is external/internal hydrostatic pressure (Sintef 1 (2017)).

Chapter 3

Fatigue Analysis

The following chapter will present theory related to fatigue estimations and calculations. This includes information for SN-curves, Miner-Palmgren summation, load history and cycle counting to mention some of the themes. The presented chapter is mainly based and taken from *fatigue handbook* (Almarnaess (1985)), the compendium *Fatigue and Fracture Design of Marine Structures* (Berge (2006)), and rules & regulations given by DNVGL-RP-0142 (2015) about wellhead fatigue analysis method.

3.1 Fatigue Damage

Fatigue is caused by cyclic loads where the loads normally are smaller than the yield stress of the material. Each cycle may be quite insignificant, and it can be impossible to detect a crack even with sensitive instrumentation. However, a load history with a number of cycles in the order of 10^8 may damage the structure so much that the integrity is threatened. The fatigue history can be divides into three stages which are associated with number of cycles. The total fatigue life is described and calculated as:

1. Initiation N_i,
2. Crack growth N_g,
3. Final failure.

$$N = N_i + N_g \tag{3.1}$$

When investigating the different stages for fatigue, there is a difference between machined components and welded joints. For machined components with a smooth surface the initial stage is dominating, while for welded joints there will be weld defects and the crack growth stage is therefore the dominating phase. Crack initiation for wellhead systems are usually present from manufacturing, and the cyclic loading leads to crack growth and failure. Important parameters to avoid weld defects are proper choice of materials, inspection, quality control systems, welding procedures and good workmanship. Welding is often done manually with covered electrodes, and during welding some kind of defects will almost be impossible to avoid. Different weld defects will give different geometry. For slag inclusions the geometry will have a more rounded shape, while for a crack and lack of fusion defects the geometry will have a sharper end. A rounded geometry is the preferred between these two due to stress distribution (Anderson (2017)). The crack growth rate curve in Figure 3.1 shows the different regions of crack growth.

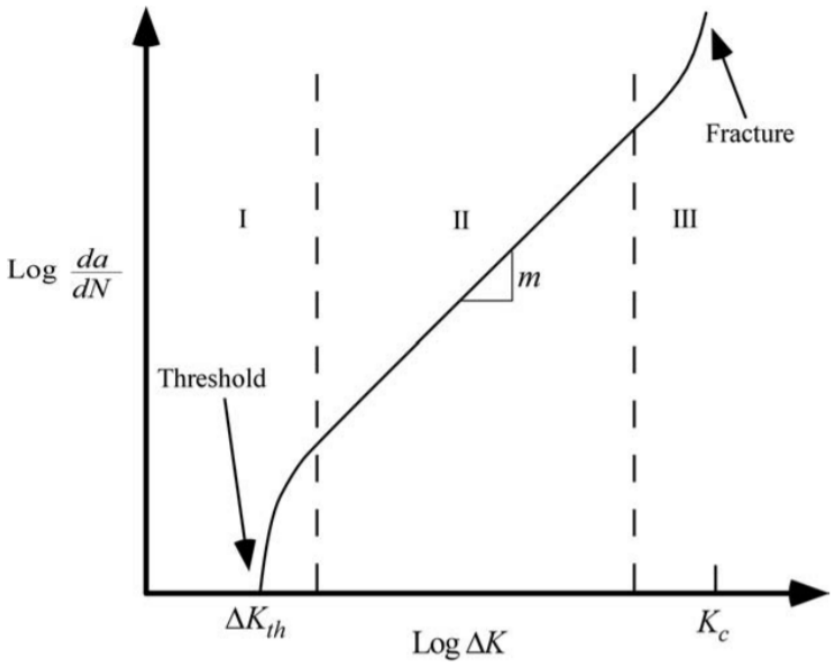

Figure 3.1: Typical fatigue crack growth behavior in metals (Anderson (2017)).

At the low end of curve, log da/dN approach zero at a threshold value of ΔK_{th}. Having a threshold value below thislimit will make the material stable, and the crack will not grow. Threshold values above ΔK_{th} will make the crack grow. The linear region, which is the interesting section considering fatigue can be described by a power law:

$$\frac{da}{dN} = C\Delta K^m \tag{3.2}$$

where C and m are material constants that are determined experimentally. ΔK is the stress intensity factor range. The crack growth rate is therefore only depending on this value.

3.2 Load History

The load history for a structure will have a history with variable amplitude which can be calculated from dynamic analyses (Almarnaess (1985)). The variable loads on a structure comes from environmental forces such as wind, currents and waves. The load history for a system is divided into blocks depending on the load range. Figure 3.2 shows the terminology used for irregular loading histories, with the most important terminologies described below the figure.

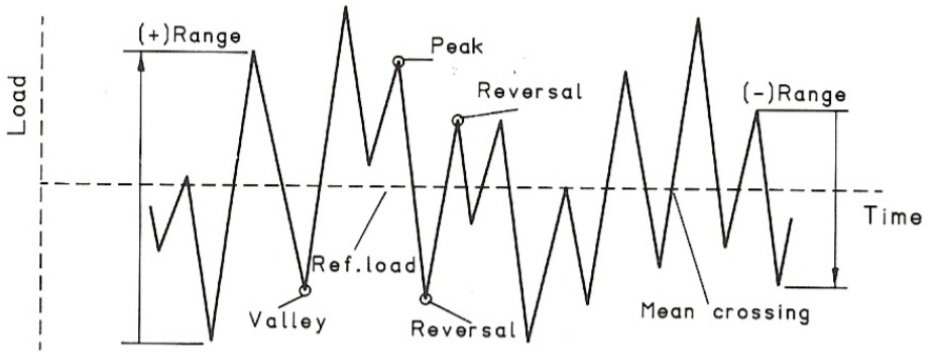

Figure 3.2: Definition of terms related to irregular load histories.

- *Reversal* first derivative of the load-time history changes sign.
- *Peak* first derivative of the load-time history changes from positive to negative sign.
- *Valley* first derivative of the load-time history changes from negative to positive sign.

- *Range* is the difference between successive valleys and peak loads (positive range) or the opposite (negative range). Note that the defined range depends on the counting method.
- *Mean crossing* is defined as the number of times that the load-time history crosses the mean load level during a given time period. Usually the crossing with only positive slopes are counted.

3.3 S-N Curve

A S-N curve is a plot of the magnitude of an alternating stress versus the number of cycles to failure. The S-N curve is obtained from fatigue tests and can be described as (Almarnaess (1985)):

$$N(\Delta S)^m = a \tag{3.3}$$

where m and a are constants, N are the number of cycles and ΔS is the stress range.

Most of the S-N data are collected by fatigue testing of small specimens in test laboratories. For a simple test specimen, the testing is performed until failure (DNV-C203 (2016)). There are several different classes for welded joints which give different S-N curves. Depending on the following criterion's listed below, a joint will first be placed in a class before a S-N curve is determined (DNV-C203 (2016)). It is possible for a structure that different joints have different S-N curves. Hence, each joint needs to be considered independently.

- The geometrical arrangement of the detail.
- The direction of the fluctuating stress relative to the detail.
- The method and inspection of the detail.

As already mentioned, each spot and geometry in a structure should be classified separately. To determine loads and their magnitude at each spot is of great importance in the design phase of a project.

The S-N curve can according to DNV be written as:

$$logN = log\bar{a} - mlog\Delta S \tag{3.4}$$

Using the SN-curve in the design phase for a structure, the mean curve should be deducted two standard deviations:

$$log\bar{a} = loga - 2\sigma_{logN} \tag{3.5}$$

If the applied stress level is below the endurance limit of the material the structure is said to have an infinite life. In other words, a crack will not grow below this value. This is introduced in the S-N curve as fatigue limit, and can be seen in Figure 3.3 (Jeddi and Palin-Luc (2018)).

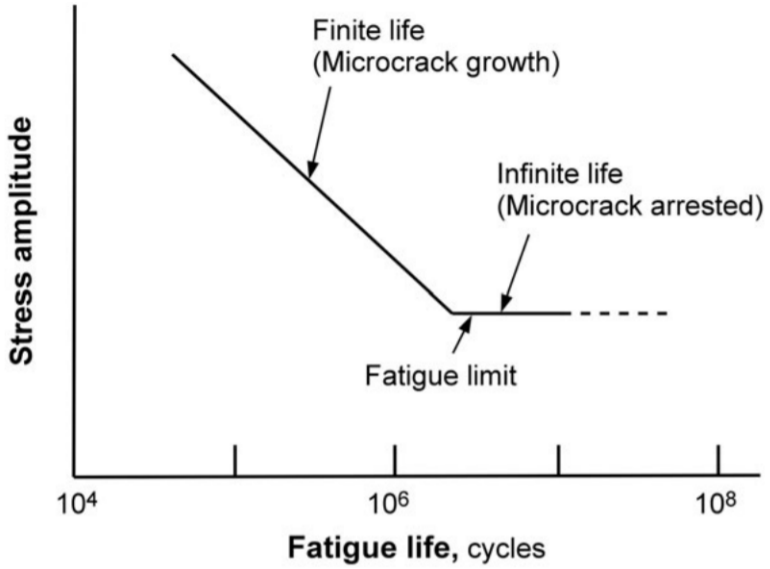

Figure 3.3: Traditional concept of S-N curve according to ASTM and AFNOR standards (Jeddi and Palin-Luc (2018)).

For welded joints, the thickness will have an impact on the fatigue life. The local geometry at the weld toe in relation to the adjoining plates will reduce the fatigue life if the plate thickness is larger than the reference thickness. The modified S-N curve with plate thickness as a factor becomes:

$$logN = loga - mlog\left(\Delta S\left(\frac{t}{t_{ref}}\right)^{k}\right) \tag{3.6}$$

where t_{ref} is the reference thickness, t is the thickness and k is the thickness exponent on fatigue strength. The local geometry can also have an impact on the stress magnitude. This is added as a stress concentration factor(SCF), and is typically located around holes or sharp edges. Calculations for the nominal stress including the SCF is according to DNV-C203 (2016):

$$\Delta S = \Delta S_{nominal} \cdot SCF \tag{3.7}$$

A stress concentration factor may be defined as the ratio of hot stress range over nominal stress range. Fabrication tolerances increases the stress range at butt

welds, but some are already included in the S-N curve. The welds in a wellhead are tubular welds, and from DNV standard RP-C203 the following equation can be used for a tubular joint with eccentricities:

$$SCF = 1 - \frac{6(\delta_t + \delta_m - \delta_0)}{t} \frac{1}{1 + \left(\frac{T}{t}\right)^{\beta}} e^{-\alpha} \tag{3.8}$$

where
δ_m = maximum misalignment
δ_t = 1/2(T-t) eccentricty due to change in thickness.
δ_0 = 0.1t is misalignment inherent in the S-N data for butt welds and analysis procedure for plated structures with an expected fabrication tolerance that is lower than that allowed in fabrication specification. The α and β values can be calculated as:

$$\alpha = \frac{1.82L}{\sqrt{Dt}} \cdot \frac{1}{1 + \left(\frac{T}{t}\right)^{\beta}} \tag{3.9}$$

$$\beta = 1.5 - \frac{1.0}{log\left(\frac{D}{t}\right)} + \frac{3.0}{\left(log\left(\frac{D}{t}\right)\right)^2} \tag{3.10}$$

Figure 3.4 shows the preferred transition in thickness of a tubular butt weld when welding is performed from the outside.

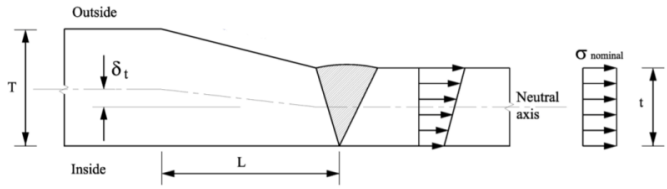

Figure 3.4: Transition in thickness at butt weld in tubular when welding only from the outside (DNV-C203 (2016)).

Figure 3.5 shows the cross section through the weld with δ_m as the maximum misalignment. As shown in Equation 3.7, it is beneficial to have a small value as possible for the SCF.

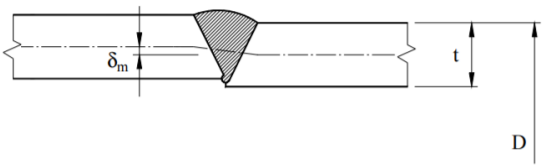

Figure 3.5: Transition in thickness at butt weld in tubular when welding only from the outside (DNV-C203 (2016)).

3.3.1 S-N curves for Variable Amplitude Loading

The S-N curve in Figure 3.3 represents structures subjected to constant amplitude loading. This is not always the case, and often some cycles will have an amplitude exceeding the fatigue limit. The values above the fatigue limit will contribute to crack growth, and the fatigue limit will be reduced with more cycles being able to exceed the lowered fatigue limit. To account for this, Haibach proposed a model with a flatter slope of factor 2*m*-1 to adjust the curve (Lee et al. (2011)). The result is a bi-linear S-N curve shown in Figure 3.6. Note that *m* is replaced with *k* in the figure.

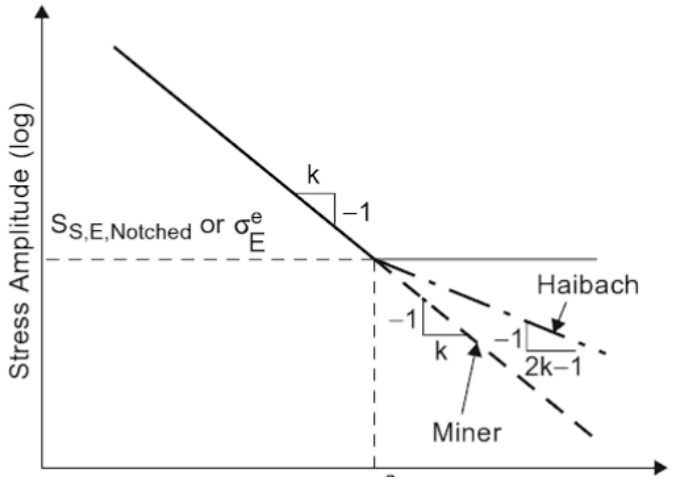

Figure 3.6: Bi-linear S-N curve (Lee et al. (2011)).

3.4 Cycle counting

There are several different methods for counting variable amplitude loading stress histories, such as the simple range counting method, peak counting, and the rainflow counting method. The rainflow counting method is the preferred one when considering low cycle fatigue. This method gives a realistic description of the physical process (Næss et al. (1985)). The intention with the *rainflow* method is to consider the history of stress/strain-time as rain flowing down a pagoda roof. The rules of rainflow counting are as follows (Næss et al. (1985)):

- Rain will flow down the roof initiating at the inside of each peak or valley. When it reaches the edge, it will drip down.
- The rain is considered to stop and a cycle is completed when it meets another flow from above.
- Starting from a peak, the flow also stops when it comes opposite a more positive peak than that from which it started. Starting from a valley, the flow stops when it comes opposite a more negative valley than that from which it started.

Figure 3.7 shows a rainflow plot based on the rules listed above. The plot is divided into stress ranges based on their stress difference. For example, the range from A-B is equal to 3 and is counted as a half cycle. The range from E-F has a value equal to 4, but is considered has a whole cycle (Irvine (2010)).

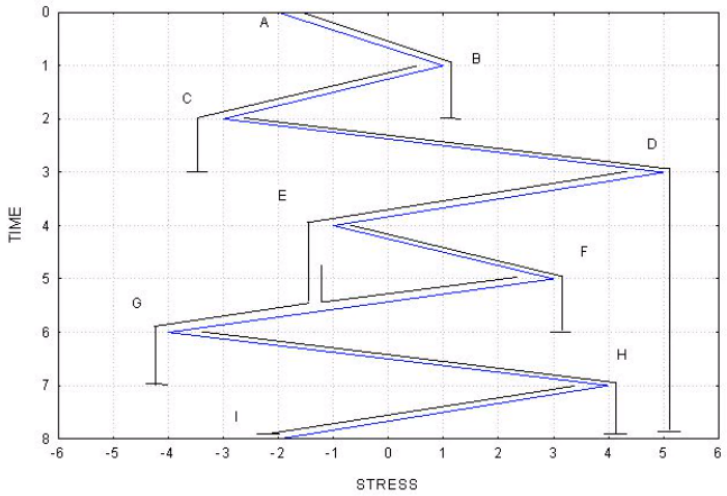

Figure 3.7: Rainflow plot (Irvine (2010)).

3.5 Cumulative Damage - The Miner Palmgren Summation

The most common method to calculate cumulative fatigue damage despite the fact that it is not consistently agree with experiments is the Miner-Palmgren summation (Sevillano et al. (2016)). Miner-Palmgren assumed that the damage on a structure per cycle with given a constant stress range can be denoted as (Næss et al. (1985)):

$$Df = \frac{1}{N} \tag{3.11}$$

where N is the number of cycles until failure at a given stress range, and D_f is the failure criterion. D_f is experimentally found between 0.7 and 2.2, but usually assumed to be 1 for design purposes (Shigley (1989)). For a structure with a complex loading in form of different stress ranges where ΔS_i contributes with n_i cycles, the Miner-Palmgren becomes:

$$\sum_{i=1}^{k} \frac{n_i}{N_i} = D_f \tag{3.12}$$

Where N_i is the number of cycles to failure with the given stress range ΔS. Combining this equation with the one for the S-N curve, Equation 3.3, the expression for damage becomes:

$$D_f = \sum_{i=1}^{k} n_i (\Delta S_i)^m \tag{3.13}$$

Normally a design fatigue factor(DFF) is introduced to reduce the probability of failure. The value of DFF value is depending on the consequences of failure and the availability for inspection. For offshore structures with safety critical components that cannot be inspected, a DFF value of 10 is required (DNVGL-RP-C203 (2016)). The modified failure criterion with DFF becomes:

$$\sum_{i=1}^{k} \frac{n_i}{N_i} = \frac{1}{DFF} \tag{3.14}$$

With a DFF equal to 10 makes it possible to rearrange the equation:

$$Df \cdot DFF < 0.1 \tag{3.15}$$

As this chapter has described, fatigue is an issue due to cycle-by-cycle loads. The stress and strain will depend on previous cycles and their values. This is called stress memory effect, and the Miner-Palmgren summation is not able to account for this. Hence, the Miner summation may be biased and can be an unpredictable manner leading to uncertainties in the calculations regarding fatigue strength and life. To ensure that the Miner-Palgren summation can be used in the design phase, a value for offshore structures for D equal to $D<0.5$ has been assessed from collection of data. The DFF is determined by the the designer, and it is therefore possible, if necessary, to select and add an additional safety factor with the Miner-Palmgren method when estimating fatigue life (Almarnaess (1985)).

Chapter 4

Riser Analysis

A riser system used offshore needs to be able to cope with both static and dynamic forces. The system will experience complex loads from currents, waves and rig motions. The need for an appropriate analysis method is necessary to have a reliable system and to establish a safety margin. Before any operation offshore that might have a consequence for the environment, several analyses are carried out to establish limitations and operation conditions. Today, these analyses are done by using the finite element method.

The following chapter introduces the theory which the RIFLEX software is based on. The chapter is mainly written in accordance with the user- and theory manual for the software. The manuals have been seen in context with *Finite element modelling and analysis of marine structures* compendium (Moan (2003)), and the book *Dynamic analysis of constructions* (Langen and Sigbjörnsson (1979)).

4.1 Static Analysis

A static analysis is performed to obtain nodal displacement to ensure that the system is in static equilibrium. The riser system will be exposed to both axial and lateral loads, with axial loading of the system containing buoyancy, top tension in the riser and weight of the components. Lateral loads working on the system will be offset of the top of the riser, currents and other specified lateral point loads. The equation for static equilibrium can be written as (Moan (2003)):

$$Kr = R \tag{4.1}$$

where K is the total stiffness matrix of the system, r is the nodal displacement vector of all degree of freedom for the system and R is the total system load

vector. The equation can also be written with the stiffness matrix as an internal structural reaction force vector and on a differential form as (Moan (2003)):

$$\mathbf{K(r)}r = \mathbf{R} \tag{4.2}$$

$$\underbrace{\frac{d}{dr}(\mathbf{K(r)r})}_{\mathrm{K}_I(r)} dr = \mathbf{dR} \tag{4.3}$$

Where $\mathbf{K}_I(r)$ is the tangential stiffness as a combination of external ($\mathbf{K}_E$), material ($\mathbf{K}_M$) and geometry ($\mathbf{K}_G$) stiffness matrices.

$$\mathbf{K}_I = \mathbf{K}_M + \mathbf{K}_G + \mathbf{K}_E \tag{4.4}$$

4.1.1 Euler-Cauchy Incremental Method

If a system is experiencing non-linear behaviour, numerical procedures is needed to solve the problem. Unlike linear problems, non-linear can experience several solutions. Hence, the obtained solution might not be the wanted one. In (Moan (2003), there are mentioned three different techniques in order to solve non-linear static response. The three techniques are as follows:

- Iterative procedures,
- Incremental or stepwise procedures, and
- Combined methods.

In RIFLEX, an incremental-iterative procedure with Euler-Cauchy incrementation is used to find static equilibrium for non-linear equation systems. Non-linear problems is often the case for slender marine structures such as risers due to large current forces. The load may be incremented up to the desired level by stepwise loading, and the displacement for each step will be added together to obtain total displacement. The load increment m+1 can be expressed as:

$$\begin{aligned} \Delta R_{m+1} &= R_{m+1} - R_m \\ \Delta r_{m+1} &= K_1(r_m)^{-1} \Delta R_{m+1} \\ r_{m+1} &= r_m + \Delta r_{m+1} \end{aligned} \tag{4.5}$$

The Euler-Cauchy does not fulfill the equilibrium in Equation 4.1. This can be seen in Figure 4.1 where the true variation and the calculated result using Euler-Cauchy method is shown. The accuracy can be improved by reducing the load increment. Hence, the load increment should be adjusted to match the degree of non-linearity.

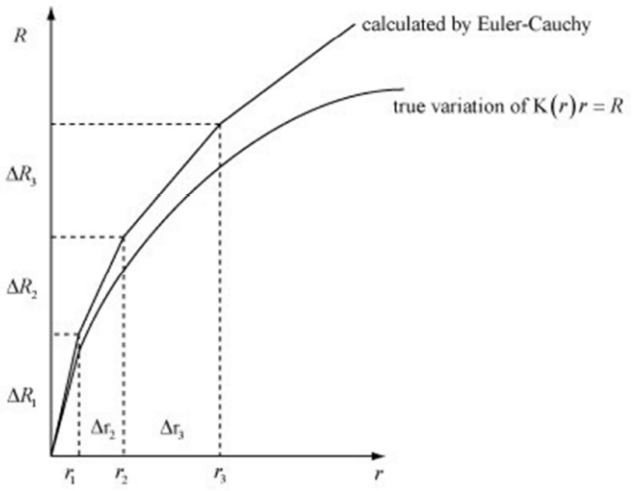

Figure 4.1: True variation compared with calculated Euler-Cauchy method.

The static configuration computed at the previous load step creates the start values for the equilibrium iteration. Correction of the displacement vector at interaction cycle *j* is given by:

$$ {}_{\Delta}r_k^0 = -\left[\frac{\partial R_{k-1}}{\partial r}\right]^{-1}(R_{k-1}^S - R_K^E) \tag{4.6} $$

$$ r_k^0 = r_{k-1} -_{\Delta} r_k^0 \tag{4.7} $$

Where ${}_{\Delta}r$ is the growing displacement vector, $\partial R/\partial r$ is the Jacobian matrix with k and $k-1$ as loads steps.

4.1.2 Iterative Methods

The most common iterative method is the Newton-Raphson method, and RIFLEX uses this approach due to the method's quadratic convergence rate. This method is based on an algorithm to solve x for the problem $f(x) = 0$:

$$x_{n+1} = x_n - \frac{f(x_n)}{f'(x_n)} \tag{4.8}$$

where $f'(x_n)$ is the derivative of $f(x_n)$ at $x = x_n$ with respect to x.

In the following equation the iteration cycle number is denoted j. For correction of the displacement vector at interaction cycle j, the expression is as follows:

$$_{\Delta}r_k^j = \left[\frac{\partial R_{k-1}}{\partial r}\right]^{-1} R_k^{j-1} \tag{4.9}$$

$$r_k^j = r_k^{j-1} -_{\Delta} r_k^j \tag{4.10}$$

It is necessary with a reliable convergence criterion to know whether the iteration should be terminated or not. In RIFLEX, the iteration is terminated when the convergence criterion is satisfied as:

$$\frac{||\Delta r_k^j||}{||r_k^j||} < \epsilon \tag{4.11}$$

where ϵ is a specified tolerance requirement which is an input parameter. It is important to have small enough load steps to avoid numerical instability that will cause small incremental rotation. Error messages within the static module are often due to this problem.

The Newton-Raphson method recomputes the stiffness matrix, *K*, at each iteration cycle. This can be time consuming, and an efficient way to improve the duration time of the analysis is to keep the *K* constant at each iteration cycle. The disadvantage is that the convergence rate will be lower. Still, this method can provide saved computational time due to the constant matrix stiffness, *K*. Figure 4.2 shows a Newton Raphson iteration, while Figure 4.3 shows the difference between using a constant *K* and updating *K*.

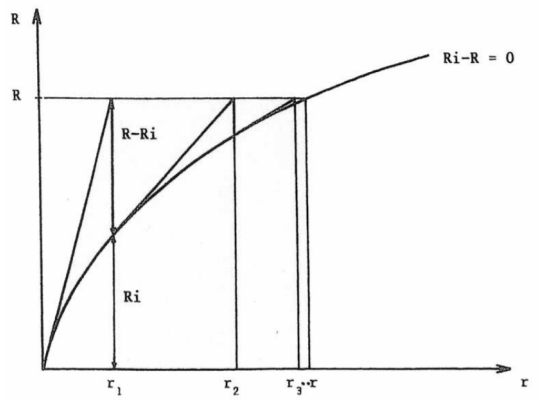

Figure 4.2: Newton-Rapshon iteration (Moan (2003)).

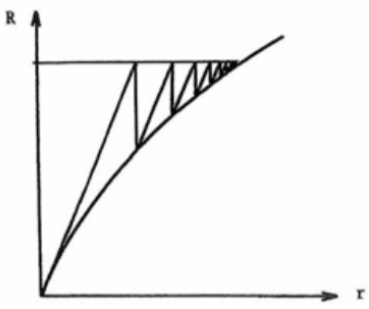

(a) Constant stiffness, *K*.

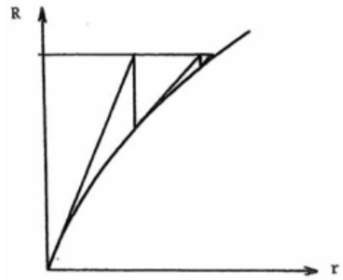

(b) Updated stiffness, *K*.

Figure 4.3: Modified Newton-Rapshod method for single d.o.f. (Moan (2003).

4.1.3 Dynamic Analysis

Unlike static analyses, dynamic analyses has time as an additional dimension. Hence, dynamic behaviour of structures can be described by displacements, velocities and accelerations. In some cases the dynamic amplification factor (DAF) can be used in static calculations to include the effect from dynamic forces. The following equation is the dynamic equilibrium that includes all motion for all degrees of freedom in the system. The equation and theory are found in the work of Langen and Sigbjörnsson (1979).

$$M\ddot{r} + C\dot{r} + Kr = R(r) \tag{4.12}$$

where r, $\dot{r}$ and $\ddot{r}$ are displacement, velocity and acceleration, respectively. M is the mass matrix and the term $M\ddot{r}$ represents inertia forces including both structural and added hydrodynamic mass. The second term, $C\dot{r}$, is the dampening matrix. This is when energy dissipates from the system. This can for example be friction, hydrodynamic damping, or plastic deformation of the material. K is the global stiffness matrix, and the term Kr represents the restoring force. The term on the right hand side of Equation 4.12, $R(r)$, is the load vector. According to the equation, the external loads are balanced by inertia, dampening and restoring forces.

RIFLEX can provide two solutions to the dynamic equilibrium equation, frequency domain and time domain. Since it is of interest to investigate the time domain, the frequency domain is not presented, only the time domain.

4.1.4 Numerical Time Integration

RIFLEX uses a step by step numerical integration of the incremental dynamic equation to solve Equation 4.12 with a Newton-Rapshon type of equilibrium at each time step. Required time for the analysis is divided into equal sub-intervals with a length h. Values for the start of a new step can be retrieved from previous time step. Necessary values for a new step are displacement, velocity and acceleration. Values at the end of a time interval can be estimated by compute the variation of the motion to the time interval. These computed results can be used as the start values for the next increment. Hence, with a large time step the accuracy decreases, with a short time step the accuracy increases.

The Newmark β-family including the Wilson θ-method with a constant time step is the foundation for the step-by-step integration in RIFLEX. These methods can

be applied for linear as well as nonlinear analyses. By comparison of the two methods, the Newmark method with β=1/4 gives the most accurate results. The Wilson method provides better results for acceleration and velocity, but has a greater period error and also a significant artificial damping.

The mentioned methods apply the relations between displacement, velocity and acceleration vectors at time t and $t + \Delta\tau$ as follows:

$$\begin{aligned} \dot{\mathbf{r}}_{t+\Delta\tau} &= \dot{\mathbf{r}}_t + (1-\gamma)\ddot{\mathbf{r}}_t\Delta\tau + \gamma\ddot{\mathbf{r}}_{t+\Delta\tau}\Delta\tau \\ \mathbf{r}_{t+\Delta\tau} &= \mathbf{r}_t + \dot{\mathbf{r}}\Delta\tau + \left(\tfrac{1}{2} - \beta\right)\ddot{\mathbf{r}}(\Delta\tau)^2 + \beta\ddot{\mathbf{r}}_{t+\Delta\tau}(\Delta\tau)^2 \end{aligned} \tag{4.13}$$

where $\Delta\tau = \theta\Delta t$ and $\theta \geq 1.0$. γ, β and θ are parameters in the integration methods defining the functional change in displacement, velocity and acceleration vector over the time step Δt. The Newmark method is unconditionally stable if the following requirements are satisfied:

$$\gamma \geq \frac{1}{2} \tag{4.14}$$

$$\beta \geq \frac{1}{4}(\gamma + \frac{1}{2})^2 \tag{4.15}$$

For situations where β is smaller in Equation 4.15, the method is only conditionally stable. The value of γ determines the artificial damping of the method (Langen and Sigbjörnsson (1979)):

$\gamma \leq 1/2$: Negative artificial damping. With increasing k the amplitude will decrease.

$\gamma = 1/2$: No artificial damping.

$\gamma \geq 1/2$: Positive artificial damping. With decreasing k the amplitude will increase.

To ensure second order accuracy, a value of $\gamma = 1/2$ is normally used.

4.1.5 Time Domain

After choosing the step by step numerical integration method, the procedure including equilibrium iteration can be described as follows:

1. Establish integration constants based on the integration parameters β, γ and θ,
2. Establish initial conditions,
   $\mathbf{r}_0 = \mathbf{r}_{\text{static}}$
   $\dot{\mathbf{r}}_0 = 0$
   $\ddot{\mathbf{r}}_0 = 0$,
3. Calculate the effective stiffness matrix, $\hat{\mathbf{K}}_{\mathbf{t}}$,
4. Calculate the effective load vector, $\Delta\hat{\mathbf{R}}_{\mathbf{t}}$,
5. Compute the incremental displacement, $\Delta\mathbf{r}_{\mathbf{t}}$,
6. Calculate velocity, $\dot{\mathbf{r}}_{\mathbf{t+\Delta\tau}}$, and acceleration, $\ddot{\mathbf{r}}_{\mathbf{t+\Delta\tau}}$,
7. Equilibrium iteration:
   (a) Set:

   $${}^{0}\Delta\mathbf{r}_{\mathrm{t}} = \Delta\mathrm{r}_{\mathrm{t}}$$

   $${}^{0}\dot{\mathbf{r}}_{\mathbf{t+\Delta\tau}} = \dot{\mathbf{r}}_{\mathbf{t+\Delta\tau}}$$

   $${}^{0}\ddot{\mathbf{r}}_{\mathbf{t+\Delta\tau}} = \ddot{\mathbf{r}}_{\mathbf{t+\Delta\tau}}$$

   $${}^{0}\Delta\mathbf{r}_{\mathrm{t+\Delta\tau}} = \Delta\mathbf{r}_{\mathrm{t+\Delta\tau}}$$

   (b) Based on the tangential mass, damping and stiffness matrices at iteration, *i-1*, establish the effective stiffness matrix, $\hat{\mathbf{K}}_{\mathbf{t}}$.
   (c) Calculate the effective residual load vector.
   (d) Compute the additional displacement increments, ${}^{\mathbf{i}}\Delta_{\mathbf{r}}$.
   (e) Calculate the improved displacement increment, ${}^{\mathbf{i}}\Delta\mathbf{r}_{\mathbf{t}}$.
   (f) Calculate displacement, velocity and acceleration as ${}^{\mathrm{i}}\mathbf{r}_{\mathrm{t+\Delta\tau}}$, ${}^{\mathrm{i}}\dot{\mathbf{r}}_{\mathrm{t+\Delta\tau}}$ and ${}^{\mathrm{i}}\ddot{\mathbf{r}}_{\mathrm{t+\Delta\tau}}$, respectively.
   (g) Perform convergence test. If the test fails, retry from (b).

4.2 Element formulation

The RIFLEX software uses finite element modelling as basis for the structural analysis part. Formulation based on small strain approximation is the reason for application to slender marine structures like risers. Other important features included in the basic finite element formulation are beam and bar elements, nonlinear material, unlimited rotation and translation in 3D space. RIFLEX has the possibility to run analyses with two dimensional beam elements as well as three dimensional elements. Figure 4.4 shows a 3D beam element with 12 degrees of freedom.

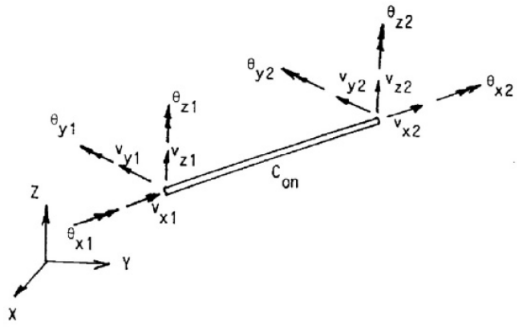

Figure 4.4: 3D beam element with 12 degrees of freedom (Sintef 1 (2017)).

The Lagrangian description is used to describe the motion of material particles, and the motion of the particles is referred to a fixed global coordinate frame. However, it might be beneficial to relate the material particles motion to a local, rectangular coordinate frame in the body. As a result, the material particles translates and rotates along with the average motion of the body. Total motion is found by a combination of the motion to a local position vector and the motion of the local reference system. Figure 4.5 shows how the motion of a material particle moves in space.

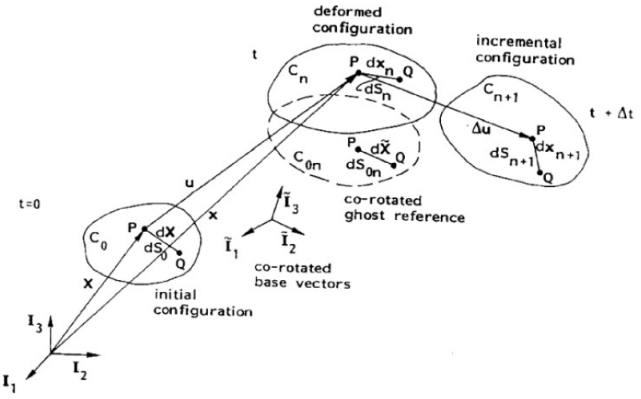

Figure 4.5: Material particle motion in space (Sintef 1 (2017)).

To express the equilibrium for a finite body, RIFLEX uses the virtual work equation. By using Piola- Kirchhoff-stressess and Green strain, the equation can be written as:

$$\int_{V_0} \mathbf{S} : \delta\mathbf{E} dV_0 = \int_{A_0} \mathbf{t}_0 \cdot \delta\mathbf{u} dA_0 + \int_{V_0} \mathbf{f}_0 \cdot \delta\mathbf{u} dV_0 \tag{4.16}$$

where V_0 and A_0 express the volume and surface of the initial reference configuration, and δ express the virtual quantities. The body forces, f_0, and the surface traction, t_0, are referred to a unit volume and a unit surface in the initial reference state.

To solve non-linear problems, most solution procedures use a linearized incremental form of the equilibrium equations. Two neighbouring equilibrium configurations can be used to establish the equation. As seen in Figure 4.5, C_n and C_{n+1} are examples of neighbouring configurations. The incremental equations can be expressed by using an incremental form of the virtual work principle as:

$$\int_{V_0} (\mathbf{S} : \delta\Delta\mathbf{E} + \Delta\mathbf{S} : \delta\mathbf{E}) dV_0 = \int_{A_0} \mathbf{t}_0 \cdot \delta\mathbf{u} dA_0 + \int_{V_0} \mathbf{f}_0 \cdot \delta\mathbf{u} dV_0 \tag{4.17}$$

Where Δ is used to denote finite but small increments between C_n and C_{n+1}. The second term in Equation 4.17 is the basis for the material stiffness matrix, and it depends in the incremental material law. The geometric stiffness matrix depends on the current state of stress, S, in the first term of Equation 4.17.

The following tangential stiffness relation for the element is derived from the incremental form of the virtual work principle given in Equation 4.16.

$$\Delta S_{int} = k\Delta v = (k_G + k_M)\Delta v \tag{4.18}$$

where Δ_{int} denotes the internal load vector in increments. k_G and k_M denote geometric and material stiffness matrices, respectively. Δv is the incremental displacement vector. The total stiffness matrix can be found as the sum of material and geometric stiffness matrices as: $k = k_G + k_M$. If it is necessary, transformation matrices can be used to transform the stiffness for an element to a global system.

As previously stated, RIFLEX use Green strain which can be given as:

$$\epsilon_G = \frac{1}{2}\left(\frac{l^2 - L^2}{L^2}\right) \tag{4.19}$$

where L is the initial length and l is the final length. Considering a beam element with a fixed coordinate system, the displacement can be uniquely described by the displacements u, v and w of the neutral axis. If all quadratic strain terms that are zero on the x-axis are neglected and quadratic axial strain term is assumed to be negligible, the Green strain may be expressed as:

$$E_{xx} = u_{,xx} - y \cdot v_{,xx} - z \cdot w_{,xx} + \frac{1}{2}(v_{,x}^2 + w_{,x}^2) \tag{4.20}$$

It is possible to define stresses with either deformed structure or its initial configuration. Stresses referring to the initial configuration are called 2nd Piola-Kirchhoff stress, while stresses referring to the deformed structure are called Cauchy stresses. Since Green strain refers to the initial configuration, same as 2nd Piola-Kirchhoff stress, the Green strain applied to a structure match with Piola-Kirchhoff stresses. For an one-dimensional case, the Piola-Kirchoff stress is related to the Eulerian stress as:

$$S_{xx} = \frac{\partial X}{\partial x}\sigma_{xx} = \left(1 - \frac{\partial u}{\partial x}\right)\sigma_{xx} \tag{4.21}$$

where x and X are coordinates of the deformed and initial configuration, respectively.

Chapter 5

RIFLEX Software and Analysis Models

The software program used to conduct global analyses, RIFLEX, is a special purpose program. Originally the program was developed for flexible marine riser systems, but it is capable to analyse any type of slender marine structures. In RIFLEX, structural response is always computed as global deformations and stress resultants. This means that local strains and stresses in different cross-sectional layers and materials are not considered.

This chapter will give an introduction to the RIFLEX software. It will show and explain different modules in the software as well as how to perform an analysis. The chapter is to an high extend based on the user- and theory manual for RIFLEX given by MARINTEK (Sintef 1 (2017), Sintef 2 (2017)).

5.1 RIFLEX Modules

An overview of the program structure can be seen in Figure 5.1. The figure shows the five different modules, INPMOD, STAMOD, DYNMOD, FREMOD and OUTMOD. The INPMOD must be run as the first module, while the STAMOD module is run after the INPMOD module. The first two modules are often compulsory for all analyses. The remaining modules can be run in an order that the user prefer. However, the most common way when performing full analysis is to run them in the following order, DYNMOD, OUTMOD and PLOMOD.

When performing a dynamic analysis, all modules must be included and run. A database manager simplifies the work for the user by storing necessary input data

and intermediate results. Each module will be further described in the following, and an explanation of what the various modules require and can handle of input data will be given. The FREMOD module can be used to carry out frequency domain analysis. Since this is not a part of the thesis, a further description of this module is omitted.

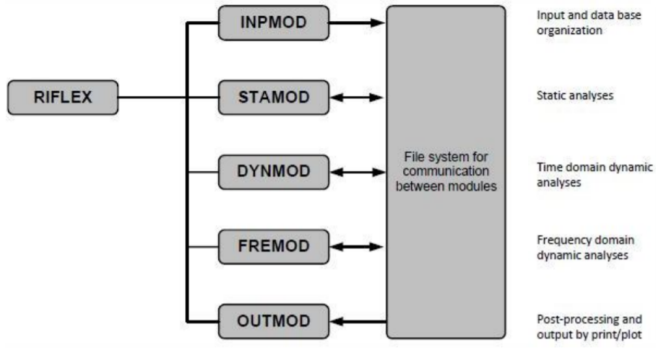

Figure 5.1: RIFLEX structure and modules.

5.1.1 INPMOD Module

The INPMOD module contains most of the input data for the analysis including boundary conditions, line and segment description, external wrapping, components like flex joints and tension ring, etc. The INPMOD module creates necessary information for the other modules.

5.1.2 STAMOD Module

The STAMOD module can run static analyses as described in Section 4.1. It is also capable to calculate the initial configuration which can be used in dynamic analysis. Element mesh, stress-free configuration and key data for finite element analyses are generated by the STAMOD module.

5.1.3 DYNMOD Module

In the DYNMOD module, a dynamic time domain analysis can be carried out based on the final static configuration, environment data and the data that defines motions applied as forced displacement in the analysis. Dynamic analysis can be

performed without rerun of INPMOD and STAMOD, and the response time series are stored as a file which can be used by OUTMOD for further post-processing.

5.1.4 OUTMOD Module

The OUTMOD module performs post-processing of the results obtained by the STAMOD and DYNMOD modules. This can for instance be time series and envelope curves for forces and moments.

5.2 Line and Segment Description

The riser system is a slender system which can be modelled by bar or beam elements. RIFLEX use super-nodes to define boundary conditions along the riser and to link different line segments together. As shown in Figure 5.2, the line consist of several different segments with a super-node at each end. The segments are then separated into several elements, and each segment can represent different cross-sectional types. Table 5.1 describes the different terms in the RIFLEX software.

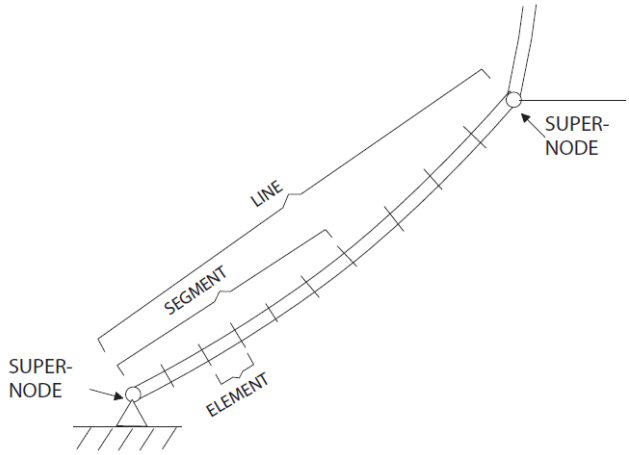

Figure 5.2: RIFLEX system definition terms.

Supernode	Points with specified boundary positions
Line	Suspended structure between two super-nodes
Segment	(Part of) line with uniform cross section properties
Element	Finite element unit

Table 5.1: Explanation of definitions in the RIFLEX software.

5.2.1 Component Description

The line shown in Figure 5.2 is build by different segments, and the segments may represent different parts and components of the riser system. By defining components with mechanical properties and attach them to a segment, the riser system can have various properties. RIFLEX has several components available, and for cross-sections the most commonly used are the Pipe cross section (CRS0) and the Axi-symmetric cross section (CRS1). They are shown in Figure 5.3 with CRS0 at the left and CRS1 at the right, respectively.

(a) CRS0 **(b)** CRS1

Figure 5.3: The CRS0 and CRS1 components in RIFLEX.

After the cross-sectional type is selected, it is specified with stiffness properties in the terms of axial and, optionally, bending and torsional stiffness. Elements with only axial stiffness are represented with 3D bar elements, while elements with axial, bending and torsional stiffness are represented with 3D beam elements. It is also possible to choose between linear and nonlinear stiffness properties for all cross-sectional types. It it however necessary to specify values for external and internal area, mass and hydrodynamic coefficients for all types.

In addition to various cross-sectional choices, nodal components can be modeled to add extra weight or buoyancy. There are a total of two different nodal components:

- Body (BODY) for modelling of clump weight, submerged buoys etc,
- Ball joint connector (CONB) for modelling swivels, hinges etc.

5.2.2 Environmental Description

The riser system is operating in a potentially harsh environment, and it is necessary to describe the environment as precisely as possible. In RIFLEX, the environment is applied in the INPMOD module. Information about water depth, currents, regular or irregular sea states and occurrence of point loads are given as input. The software offers several opportunities to describe wave loads working on the riser system. For irregular sea states, the following frequency spectrum is available, Pierson-Moscowitz, JONSWAP, Bretschneider, Torsethaugen and Derbyshire-Scott. For operations in the North Sea, the most common ones are the JONSWAP and Pierson-Moscowitz spectrum. The JONSWAP and Pierson-Moscowitz spectrum are described in more detail in Section 2.9.

5.2.3 Description of Vessel

The vessel in RIFLEX is given as a coordinate for the vessel position. A super-node is attached to the vessel, and appropriate boundary condition for the connected super-node is assigned. The rig will experience movement in different sea states. It is therefore necessary to provide a transfer function as an input to the program in order to describe and calculate the movements. It is also necessary to decide the degrees of freedom to the vessel.

5.3 RIFLEX Analysis Models

The name *riserless well intervention* may mislead the reader into believing that the RLWI operation in the analyses is without a riser. This is as stated in Section 2.7 a possibility, but the RLWI system can also be used with a riser that is smaller than for a drilling operation. The RLWI system will have a 9" riser while the drilling operation will have the traditional 21" for the analyses. Although there will be a 9" riser in the RLWI operation, the name will be kept the same throughout the thesis. The following will thoroughly describe the two systems and the differences between them.

5.3.1 Presentation of RIFLEX-models

One of the models will be based on a drilling riser system, which is an example provided by MARINTEK. The other model will be based on a RLWI system as shown in Figure 2.6. The configuration of the marine riser systems are based on a semi submersible operating in weather conditions from the Ekofisk-field in the North Sea. The RLWI system is supposed to represent an intervention job during production phase, while the drilling example is supposed to represent the drilling phase of the well.

Figure 5.4 shows of the drilling riser system in RIFLEX. The RLWI- and drilling riser system will look the same from distance. The blue and grey rectangle represents the sea surface and seafloor, respectively. In the middle of the figure at the surface, the semi-submersible is located. The green line hanging from the semi-submersible represents the riser going from the rig down to the seafloor. At the left end of the figure, there is a green graph indicating the currents speed and direction across the water depth. The blue arrow shows the wave propagation direction.

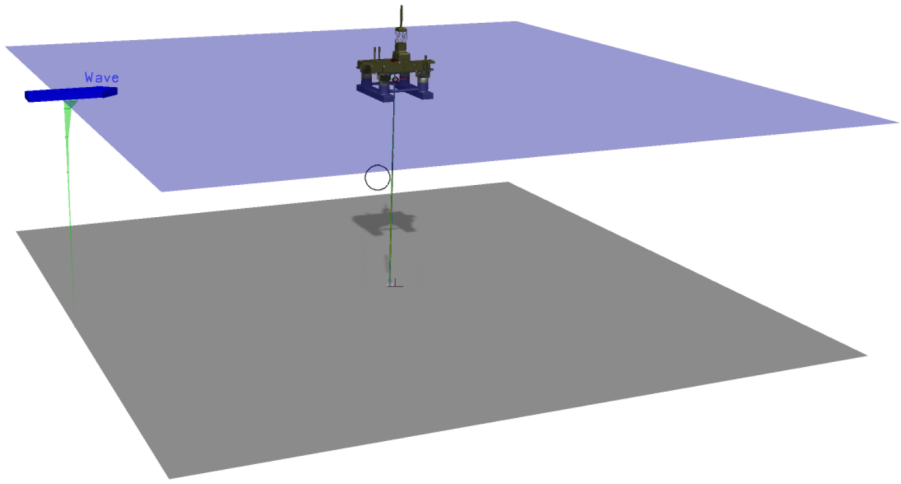

Figure 5.4: Drilling riser system with wave and currents direction.

The upper part of the risers are similar between the two models. Figure 5.5 shows a more detailed view of the components close to the semi submersible where the telescopic joint is placed before the upper flex joint. The upper flex joint is located at the top of the riser. There are in total six tensioners, and all the tensioners have a super-node at each end.

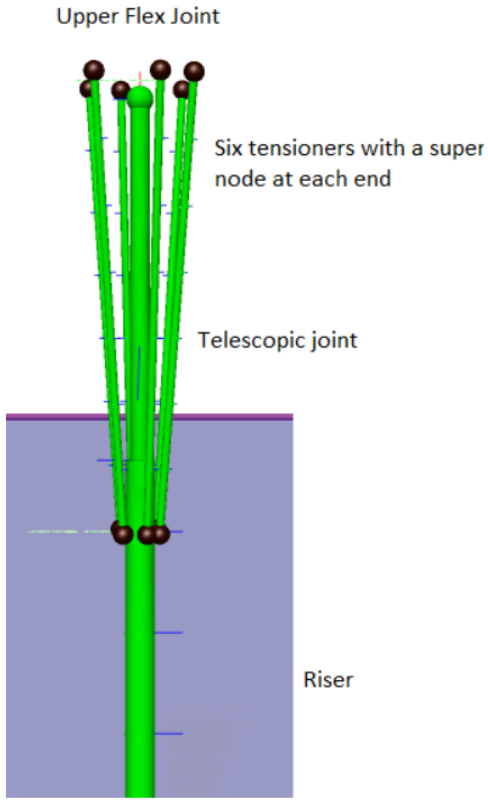

Figure 5.5: View of the components in the upper part of the risers in RIFLEX models.

The lower parts of the riser models will be slightly different from each other. As shown in Figure 5.6, the traditional system will consist of a LMRP and riser with buoyancy elements. With the intervention system, the LMRP package is substituted with a RLWI stack. The riser used in the RLWI system will have a significant smaller cross sections than the drilling riser. Hence, the weight will be much less and therefore have a lighter weight. Furthermore, it is not necessary with any buoyancy elements for 9” riser.

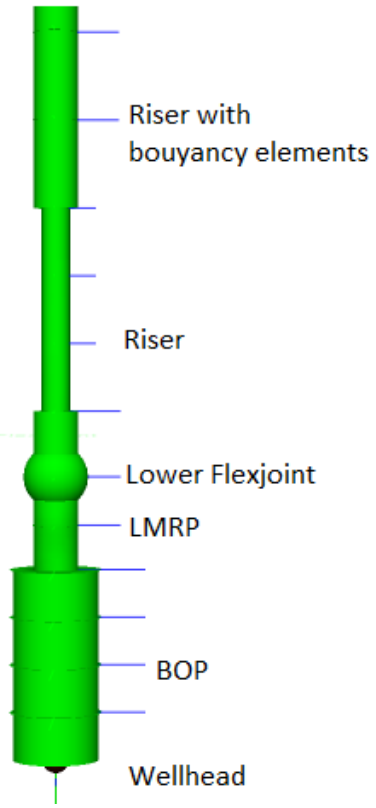

(a) Traditional drilling riser with LMRP and riser with buoyancy elements.

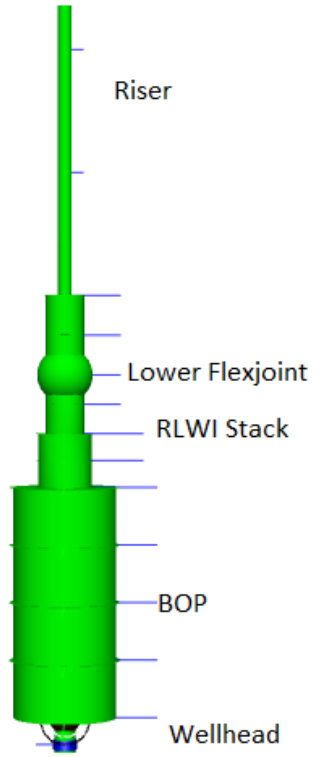

(b) Intervention marine riser system with RLWI stack.

Figure 5.6: Detailed view of the lower part of the riser models with the difference between traditional marine riser system and intervention system.

5.3.2 Structural modelling in RIFLEX

First Order Motions Function

First order functions are used to describe the semi submersible motion in the global analyses. The transfer functions are calculated in another software such as WAMIT or Wadam. The transfer functions are therefore given as input data for the analyses. Since the data only consider first order, higher order effects that might affect the force response in the system is neglected. For the analyses, the wave heading is 0 degrees. Surge and pitch motions are important for the results in the analyses because they will give the lateral displacement at the top of the drilling riser. The following figures will show the first order motion for surge and pitch, respectively. The marine riser systems will have a heave compensator system onboard the rig. Thus, heave motion should not be a concern for the forces in the riser.

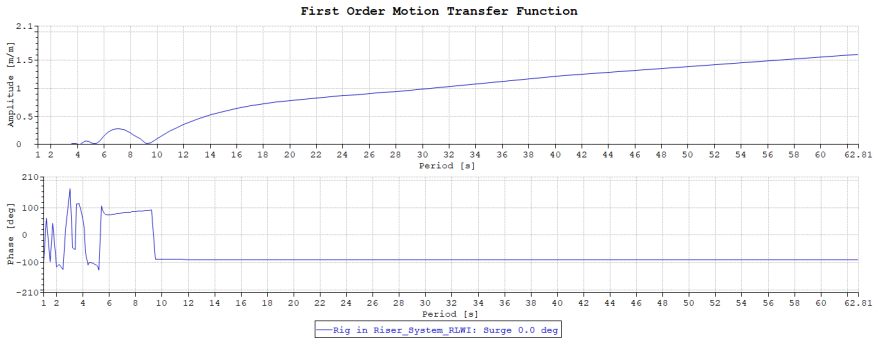

Figure 5.7: First order motions transfer function for surge, 0°.

Pitch, roll and yaw are all dimensionless and given as rotation per wave slope.

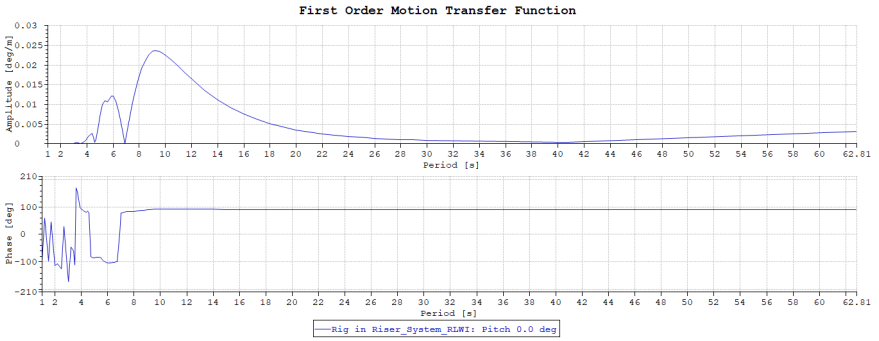

Figure 5.8: First order motions transfer function for pitch, 0°.

5.3.3 Risers

The total length of the riser sections are 315.5 metres. Where the RLWI riser consist of only one joint with a constant cross section, the drilling riser has four different joints with different properties. The drilling riser has a pup section with a length equal to 20 feet at the upper end, and 15 feet at the lower end of the riser. The RLWI system is mainly built by 50 feet long sections. However, where a shorter joints are needed that fits the water depth, shorter sections are used. In the traditional system, the riser is mainly built by slick 50 feet joints and 50 feet long buoyancy elements. Slick joint is a special riser joint designed to prevent damage to the riser and to control umbilicals where they pass through the rotary table (API RP (2016)).

Table 5.2 shows the properties to the drilling riser. There is a slight difference between the 20ft and 15ft pup sections regarding wall thickness. A reason for why they are not the same could be the fact that a fault or damage at the lower end of the riser is more critical than in the upper end.

Parameter	Slick50ft_cs	Buoyancy50ft_cs	Pup15ft_cs	Pup20ft_cs	Unit
Length	106.68	198.12	4.57	6.10	*[m]*
Wall thickness	248.00	558.70	271.10	264.80	*[mm]*
Internal diameter	502.00	527.00	527.00	527.00	*[mm]*
External diameter	750.00	1085.70	798.10	792.80	*[mm]*
Mass coefficient	361.09	558.01	503.06	442.91	$[kg/m]$
Axial Stiffness	$5.43{\cdot}10^{9}$	$5.43{\cdot}10^{9}$	$5.43{\cdot}10^{9}$	$5.43{\cdot}10^{9}$	$[Nm^2]$
Bending stiffness	$1.82{\cdot}10^{8}$	$1.82{\cdot}10^{8}$	$1.82{\cdot}10^{8}$	$1.82{\cdot}10^{8}$	$[Nm^2]$
Torsion stiffness	$1.41{\cdot}10^{8}$	$1.41{\cdot}10^{8}$	$1.41{\cdot}10^{8}$	$1.41{\cdot}10^{8}$	$[Nm^2]$
Hydrodynamic Diameter	0.76	1.11	0.76	0.76	$[m]$
Drag coeffisient	1.00	1.00	1.00	1.00	[-]
Added mass coeff.	0.82	1.10	0.82	0.82	[-]

Table 5.2: Cross section properties and length for the traditional 21” riser joints.

The RLWI riser has smaller cross sections than the drilling riser, and the weight of the sections are lighter. The 9" riser in the RLWI system will have the properties given in Table 5.3. Calculations of the properties can be found in Appendix B. The two tables for the risers shows that there is a significant difference between the them. Note especially the difference between the mass coefficient and the hydrodynamic diameters.

Parameter	RLWI_riser_9"	Unit
Length	315.50	*[m]*
Wall thickness	25.40	*[mm]*
Internal diameter	177.80	*[mm]*
External diameter	228.60	*[mm]*
Mass coefficient	127.29	$[kg/m]$
Axial Stiffness	$3.405 \cdot 10^9$	$[Nm^2]$
Bending stiffness	$1.785 \cdot 10^7$	$[Nm^2]$
Torsion stiffness	$1.373 \cdot 10^7$	$[Nm^2]$
Hydrodynamic Diameter	0.29	$[m]$
Drag coeffisient	1.00	[-]
Added mass coeff.	0.82	[-]

Table 5.3: Cross section properties and length for the 9" RLWI riser.

The weight of the riser section for the RLWI system is approximately 400 kN, while the drilling riser has a weight of approximately 1500 kN. This gives a weight difference close to 1100 kN.

5.3.4 Internal Fluid

In a drilling operation, drilling fluid is used to provide hydrostatic pressure to prevent formation fluids from entering into the well bore. The fluid also keeps the drill bit cool and clean during drilling, carrying out drill cuttings, suspending the drill cuttings while drilling is paused and when the drilling assembly is brought in and out of the hole. For the RLWI system the density might vary from 0 to 2 in s.g (specific gravity) (Sangesland (2019)). For the analyses, an internal fluid equal to $1600 kg/m^3$ is chosen for both the drilling- and the RLWI system.

5.3.5 Blow out preventor - BOP

Ideally the weight and properties of each component should be obtained from the manufacturers. This is not always possible, and it is therefore some assumptions that must be made to conduct an analysis. The BOP used in a standard drilling operation is heavy compared to the BOP used in an intervention operation. The weight of a subsea BOP has increased in recent years due to more demanding safety standards. The total weight of the heavy BOP stack is estimated to be 346 tons, while the light BOP used during intervention with the RLWI stack is estimated to have a total weight of 162.2 tons. Table 5.4 and Table 5.5 shows the properties for the different BOPs.

Parameter	bop_cs1	bop_cs2	Unit
Length	2.21	2.21	*[m]*
Mass coefficient	44076.00	44076.00	*[Kg/m]*
External cross section area	2.79	2.79	$[m^2]$
Internal cross section area	0.20	0.20	$[m^2]$
Height	4.28	4.28	$[kg/m]$
Axial Stiffness	$1.0{\cdot}10^{13}$	$1.0{\cdot}10^{13}$	$[Nm^2]$
Bending stiffness	$1.0{\cdot}10^{13}$	$1.0{\cdot}10^{13}$	$[Nm^2]$
Torsion stiffness	$1.0{\cdot}10^{13}$	$1.0{\cdot}10^{13}$	$[Nm^2]$
Hydrodynamic Diameter	4.52	4.52	$[m]$
Drag coeffisient	1.00	1.00	[-]
Added mass coeff.	1.10	1.10	[-]

Table 5.4: Properties for the heavy BOP.

Parameter	bop_cs1	bop_cs2	Unit
Length	2.21	2.21	*[m]*
Mass coefficient	19191.00	19191.00	*[Kg/m]*
External cross section area	2.79	2.79	$[m^2]$
Internal cross section area	0.20	0.20	$[m^2]$
Height	4.28	4.28	$[kg/m]$
Axial Stiffness	$1.0{\cdot}10^{13}$	$1.0{\cdot}10^{13}$	$[Nm^2]$
Bending stiffness	$1.0{\cdot}10^{13}$	$1.0{\cdot}10^{13}$	$[Nm^2]$
Torsion stiffness	$1.0{\cdot}10^{13}$	$1.0{\cdot}10^{13}$	$[Nm^2]$
Hydrodynamic Diameter	4.52	4.52	$[m]$
Drag coeffisient	1.00	1.00	[-]
Added mass coeff.	1.10	1.10	[-]

Table 5.5: Properties for the light BOP.

The stiffness of the BOP's are compared to the risers rather high. As a result the BOP's will have small deformations compared to the risers. Both BOP's are divided into two segments, but they will have the same cross section and properties throughout. Dividing the model into several segments using the same cross section might seem unnecessary. It can however be useful when e.g changing properties or running convergence studies. Between the light and heavy BOP, only the weight has changed. This is naturally not correct, and other values should be changed as well. Due to the lack of reliable sources, the other parameters are kept the same.

5.3.6 LMRP- and RLWI Stack

During a drilling operation with 21" riser and a heavy BOP, a lower marine riser package will be a part of the BOP stack. For a RLWI operation the LMRP is substituted with the RLWI stack. Estimates of mass and drag coefficients and other parameters for the RLWI stack are difficult to decide without credible sources. Currents and other environmental forces close to the seabed could potentially have significant impact on the riser systems. For this reason, the values for the LMRP stack are used for the RLWI stack, except for the hydrodynamic diameter. The hydrodynamic diameter is reduced, and the stiffness of the stack is lowered to $^{1}/_{1000}$ of the LMRP. A convergence study and further investigation of the stiffness to the stack will be investigated in the Section 8.1. Table 5.6 shows the difference between the LRMP- and the RLWI stack.

Parameter	LMRP_cs	RLWI_cs	Unit
Mass coefficient	44076	22421.5	$[Kg/m]$
External cross section area	0.74	0.74	$[m^2]$
Internal cross section area	0.20	0.20	$[m^2]$
Height	4.28	4.28	$[kg/m]$
Axial Stiffness	$1.0{\cdot}10^{13}$	$1.0{\cdot}10^{10}$	$[Nm^2]$
Bending stiffness	$1.0{\cdot}10^{13}$	$1.0{\cdot}10^{10}$	$[Nm^2]$
Torsion stiffness	$1.0{\cdot}10^{13}$	$1.0{\cdot}10^{10}$	$[Nm^2]$
Hydrodynamic Diameter	4.52	2.52	$[m]$
Drag coeffisient	1.00	1.00	[-]
Added mass coeff.	1.10	1.10	[-]

Table 5.6: Properties for the LRMP- and RLWI stack.

5.3.7 Telescopic Joint

The telescopic joint is the same for both systems. Two cylinders slide relative to each other in the telescopic joint. The inner barrel has a smaller diameter than the outer barrel, and the cylinders is modelled by using one element in the segment. The cross-sections for the two cylinders are listed in Table 5.7.

Parameter	Outer barrel	Inner barrel	Unit
Total mass	16409.94	105.5	*[kg]*
External cross section area	0.55	0.22312	$[m^2]$
Internal cross section area	0	0	$[m^2]$
Height	19.79	10.549	*[m]*
Axial stiffness	$6.22 \cdot 10^9$	10	$[Nm^2]$
Bending stiffness	$2.74 \cdot 10^8$	$1.82 \cdot 10^8$	$[Nm^2]$
Torsion stiffness	$2.121 \cdot 10^8$	$1.405 \cdot 10^8$	$[Nm^2]$
Hydrodynamic diameter	0.83	0	*[m]*
Drag coefficient	1	0	[-]
Added mass coeff.	1	0	[-]

Table 5.7: Properties for the Inner and Outer barrel at the Telescopic joint.

5.3.8 Flex joints

There are two flex joints in the riser system, one upper and one lower. Both are retrieved from the database in RIFLEX. The flex joints are modelled with zero length, but they can have properties for mass and volume. The properties for the two flex joints are listed in Table 5.8 below.

Parameter	Lower flex joint	Upper flex joint	Unit
Stiffness rotation X	Linear	Linear	
Stiffness rotation Y	Non linear	Linear	
Stiffness rotation Z	Non linear	Linear	
Damping rotation X	0	0	
Damping rotation Y	43280	0	*[Nms/deg]*
Damping rotation Z	43280	0	*[Nms/deg]*

Table 5.8: Properties for the lower and upper flex joint in both RIFLEX models

5.3.9 Tensioners

The tensioners are the only elements of the system that are modelled as bar elements and not as beam elements. Hence, the tensioners are only able to deal with axial forces. The axial force in each tension is the same as in the MARINTEK example. Figure 5.9 shows how the axial stiffness is a function of the elongation of the tensioner.

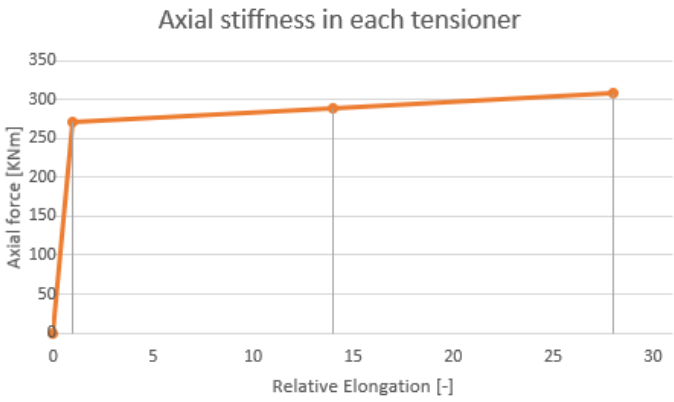

Figure 5.9: Axial stiffness in tensioners as function of relative elongation.

5.3.10 Wellhead

The wellhead is modelled as a line with beam elements. The line has a total length of 8.2 metres, and enters the soil with a length of 5.07 metres. Hence, the stick up height from the seabed is 3.1 metres. To represent the soil interaction, a non-linear spring is used for all the analyses. The soil spring is retrieved from the MARINTEK example. At the bottom of the well the boundary conditions are fixed for translations but free for rotations. At the top of the well the boundary conditions are free for both rotations and translations. Because of the free boundary conditions at the top of the well, the soil spring is important for the lateral displacement at the wellhead. Obtaining and implementing more realistic soil properties for the field is recommended.

5.3.11 Environment

The riser system will experience environmental loads that needs to be implemented in the analyses. Both current and wave loading will have an impact on the riser system. The environmental data should be gathered from measurements over a period of time to verify accuracy of the analysis results. This can usually be difficult for a oil or gas field that is under exploration or development. The environment used in the analyses is based on the Ekofisk-field, which is located about 320km southwest of Stavanger. The data used in the scatter diagram in this thesis is gathered from 1980 to 1993.

Irregular Wave Environment

Performing parametric studies a regular wave environment could be useful. The ability to change only one parameter at a time allows to easily check the differences for each analysis. However, for the fatigue analysis an irregular wave environment should be used. It is possible to determine which angles the waves are entering, spreading of the wave, wave height, peak period and so on. It is also possible to determine the parameter, *seed*, which determine the generated phase angles. By using a increased value for the seed parameter, the sea spectrum is divide into smaller parts. An increased number of seeds will therefore give more phase angles and represent the sea spectrum more accurately. The total scatter diagram of the Ekofisk-field can be seen in Table 5.9.

Table 8-8 Scatter diagram for the Ekofisk-field (Myrhaug, 2007).

Hs / Tp	<4	5	6	7	8	9	10	11	12	13	14	15	16	17	18	19	20	21	
0.5	219	247	98	56	108	139	85	53	38	28	16	9	3	1	1	1			1102
1.0	462	1444	1332	551	394	409	362	255	153	126	66	73	28	20	9	4		1	5689
1.5	54	763	1991	1654	703	436	327	258	176	86	49	49	23	21	22	3	3	3	6621
2.0	1	114	994	2015	1329	583	260	246	193	91	37	20	10	16	14	3	1		5927
2.5		7	189	1122	1532	734	261	182	165	124	48	20	8	1	1	2	1		4397
3.0			14	329	1082	958	309	137	139	96	39	13	6			1	1	1	3125
3.5				59	533	983	382	140	87	72	33	15	4	2		1			2311
4.0				10	133	660	418	144	65	36	23	14	3	4					1510
4.5					28	313	417	149	41	25	7	10	4	1					995
5.0					2	113	271	190	40	19	8	6	2	1					652
5.5						23	154	136	49	23	7	12	4						408
6.0						4	61	109	52	26	4	6	4						266
6.5							20	58	35	14	6	4	5						142
7.0							6	23	35	14	5	2	1						86
7.5							2	21	16	13	4	3	2	1	1				63
8.0								4	8	9	3	1							25
8.5								2	8	3	2	3	2						20
9.0									2	5	2								9
9.5									1	5	1	3	2						12
10.0												1							1
10.5										2	1	1		1					5
11.0											1								1
11.5										1		1		1					3
12.0												1							1
	736	2575	4618	5796	5844	5355	3335	2107	1303	818	362	267	111	70	48	15	6	5	33371

Table 5.9: Scatter diagram for the Ekofisk-field between 1980 and 1993 with a total of 208 blocks.

Performing an analysis with all the sea states in the scatter diagram is very time consuming. It is often beneficial to simplify the scatter diagram to reduce the computational effort, especially when performing several analyses. There are standards describing how to do conservatively reduce the scatter diagram. It is recommended according to API RP 17B (2008) to divide the diagram into minimum five blocks, using the maximum value of the sea state for each block. The scatter diagram for the Ekofisk field is reduced from 208 down to 58 blocks. A total reduction of 150 blocks is significant in terms of reduced computational time. The reduced scatter diagram for the Ekofisk field is shown in Table 5.10

Spectral Peak Period																	
Hs	4	5	6	7	8	9	10	11	12	13	14	15	16	17	18	19	20	21	sum
0.5				620				385				91				6			1102
1				3789				1420				345						135	5689
1.5				4462				1724				360						75	6621
2				3124				2418				341					44		5927
2.5					2850				1342				200				5		4397
3					1425				1543				154					3	3125
3.5						1575			609			120				7			2311
4						803			627					80					1510
4.5							758			215				22					995
5							386			249				17					652
5.5								362					46						408
6								226						42					268
6.5									127				15						142
7									78				8						86
7.5									52							11			63
8									21			4							25
8.5									13				7						20
9												9							9
9.5													12						12
10												1							1
10.5														5					5
11											1								1
11.5														3					3
12												1							1
																			33373

Table 5.10: Reduced scatter diagram with only 58 blocks for the Ekofisk field.

Simulation and Calculation procedure

As mentioned in Section 4.1.3, the global analyses are a time domain simulation. According to research done by Steinkjer et al. (2010), the duration of the simulation should be minimum set to 3600 seconds to avoid statistical uncertainty of more than 10%. The time step is a important parameter because it determines how often the response should be calculated in the analysis. If the time step is set too large, some of the response amplitudes may not be included. This can lead to an incomplete numerical solution. To avoid this problem, the time step is set to 0.1 seconds.

RIFLEX applies the Newmark-β procedure for non-linear analysis. Values for the integration and damping parameters for the dynamic analysis can be seen in Table 5.11.

Parameter	Value	Unit
Inverse β (Beta)	3.90	[-]
γ (Gamma)	0.505	[-]
Stiffness damping	0.03479	[-]

Table 5.11: Values for the parameter used in the dynamic calcualtions in RIFLEX.

With an inverse β close to 4, it is assumed a constant average acceleration between the time steps. A value of gamma, γ, equal to 0.5 gives zero artificial damping.

5.3.12 SN-Curve fatigue analysis

The selection of a SN-curve will have an significant impact on the fatigue calculations. For the selection of SN-curve, the standard DNV-C203 (2016) is used. The SN-curve C1 can be used for machine flushed welds, while the B1 curve can be used for plain plates without welds. To use C1 and B1, the wellhead must be completely protected from the corrosive environment. The wellhead should also be protected during transportation and storage. If this is not possible, the SN-curve F3 should be considered for the wellhead. It is assumed that the wellhead is handled gently, and that there is no weld at the area of interest. Therefore, the SN curve B1 with seawater protection is selected for the fatigue assessments. In a previous master thesis by A. Lylund, Statoil provided SN-curves. Selecting the B1 curve with seawater protection corresponds to Statoil's selections for the wellhead (Lylund (2015)).

Chapter 6

ABAQUS Software and Analysis Model

ABAQUS includes various analytical programs and can solve a wide range of engineering problems although it was first developed to solve non-linear physical behavior. ABAQUS is also capable of modelling a variety of geometries and material through its extensive element and material libraries. In Chapter 4, the finite element method for the RIFLEX software was explained. As for RIFLEX, ABAQUS is based on the finite element method. The first part of this chapter will show that the basis for the programs are much the same, and this is to a high extend based on the theory- and user manual for ABAQUS.

ABAQUS consist of three different products as listed below with a brief explanation.

- ABAQUS/Explicit - use explicit dynamic finite element formulation and is suitable for special purposes like impact and blast problems.
- ABAQUS/CAE - is useful for pre- and post-processing of graphical environment.
- ABAQUS/Standard - is a program which is capable to solve linear, nonlinear, static and dynamic problems.

For this thesis the ABAQUS/CAE product is used, and the following will be presented with this as basis.

6.0.1 ABAQUS Analysis Steps

A complete ABAQUS simulation consist of three distinct stages, pre-processing, simulation and post-processing. Figure 6.1 shows the different stages and how different file types link them together.

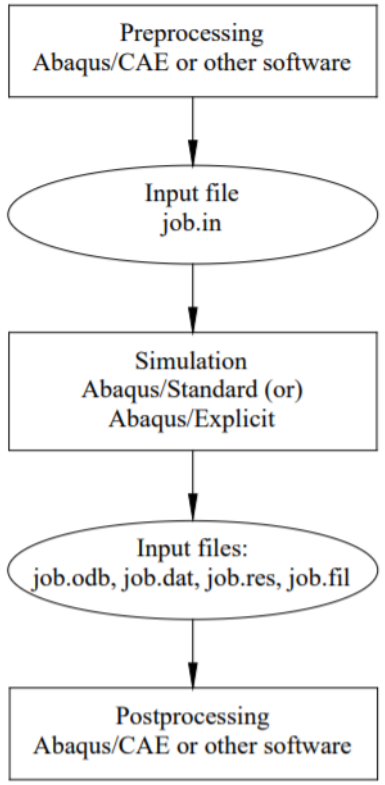

Figure 6.1: ABAQUS stages for simulation (ABAQUS (2008)).

Pre-processing
In the pre-processing stage, the model is created. After geometries with correct dimensions are built, different material properties are assigned to the created parts. Selection of elements and how the model should be meshed is also performed in the pre-processing stage. The model is then assigned appropriate boundary conditions for the given case with loads acting on the model. Loads- and boundary conditions needs to be applied with caution to correctly represent the situation and to obtain reliable results. Using the entire model rather than just a quarter or half requires less caution in assigning boundary conditions and loads.

Simulation
It is common in this stage to decide which outputs are desired from the simulation. Output variables as stresses, displacement, strains, velocities, accelerations and forces are possibly the most common ones for regular analysis. It is also possible to determine number of time steps to be stored in the solution.

Post-processing
After the simulations stage is completed, the post-processing of the results can begin. The chosen output parameters that were decided in the simulation stage can be reviewed and evaluated. As a part of the evaluation of the results, it is important to keep in mind that the analyst is responsible for all FE results. Hence, experience and knowledge is required of the analyst to perform and evaluate FE-results in a safe manner (ABAQUS (2008)).

6.1 Element formulation in ABAQUS

There are numerous types of elements within ABAQUS CAE. Examples of 2D elements may be bar, beam, shell, plates and solid elements. All elements have in common that they use numerical integration to allow complete generality in material behavior. For the analyses the element type C3D20R is used. This 3D element is representing a 20-node quadratic brick with reduced integration hsaving 3*3*3 integration points. Figure 6.2 shows the element with node numbering.

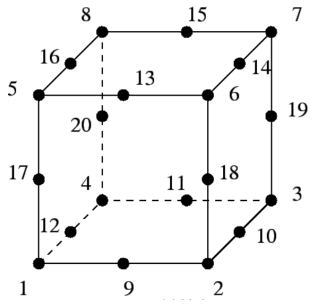

Figure 6.2: 20-node brick element (ABAQUS (2008)).

The element is suitable for linear elastic calculations. Due to the location of the integration points, the stress concentrations on the surface of a structure are well captured. For nonlinear calculations, the element experience the same problem as a lower noded element, e.g C3D8 element when using full integration. The element tends to be too stiff in bending. This problem is also known as shear locking. The problem often occurs for slender beams or thin plates. A way to avoid shear locking is to use reduced integration. It is possible to use reduced integration for quadrilateral and hexahedral elements. By using reduced integration the element is integrated with a quadrature rule of less than full order, usually one order lower than full integration. The Gauss points corresponding to reduced integration are the so-called Barlow points, also known as super-convergent points. Strains and stresses are calculated with the best accuracy for the Lagrange polynomial at the Barlow points. Some polynomial terms are zero at the Barlow points, and because of that they do not contribute with element stiffness. This may lead to improved accuracy of the results because it softens the behaviour of the element. A possible problem with reduced integration is a rank-deficient stiffness matrix, k. For a rank-deficient k , there exist one or more spurious modes of deformation that may be activated without any increase in the strain energy. These spurious modes are also known as hour-glass-modes, zero-energy-modes or element instability modes.

As for RIFLEX, ABAQUS CAE uses the virtual work equation to calculate the equilibrium for a finite body. The equilibrium equations obtained by discretizing the virtual work equation can be written as:

$$F^N(u^M) = 0 \tag{6.1}$$

where F^N is the force component conjugate to the N^{th} variable in the problem. u^M is the value of the M^{th} variable. The strain formulation in ABAQUS/CAE is the same as in RIFLEX, so-called Green strain. ABAQUS uses Lagrange elements, hence the strain is given as the Green-Lagrangian strain tensor. The strain tensor can be written as:

$$E = \frac{1}{2}(F^T \times F - I) \tag{6.2}$$

$$F^T \times F = \left(\frac{dx}{dX}\right)^T \cdot \frac{dx}{dX} \tag{6.3}$$

Where **I** is the initial condition and **F**. x is the new position vector after a displacement, while X is the initial position.

The stress measure used in ABAQUS is the same as in RIFLEX, second Piola-Kirchhoff stress tensor. Piola-Kirchhoff stress tensor can be written as:

$$S = R^T \cdot \sigma \cdot R \tag{6.4}$$

Where the components of S are the rotated axis of components of σ. R work as an orthogonal tensor, which can for example describe a rotation (ABAQUS (2008)

6.2 Static analysis in ABAQUS

The purpose of a static analysis in ABAQUS is to find a solution for static equilibrium for the system. The equilibrium equation is written as in RIFLEX, on the incremental form, and is as follows:

$$F^N(u^M) = 0 \tag{6.5}$$

6.2.1 Newton-Raphson iteration in ABAQUS

ABAQUS uses the Newton-Raphson method for numerical iteration to satisfy and solve the equilibrium equation. The main advantage of the Newton-Raphson method is the rapid rate of convergence. Analysis with a large degree of non-linearity will use the modified Newton-Raphson method as shown in Figure 4.3. ABAQUS uses a scheme based predominantly on the maximum force residuals following each iteration. The software compares the consecutive values of these quantities before it checks and verify if convergence is possible to obtain in a reasonable number of iterations. If ABAQUS detect that convergence is deemed unlikely, the load increment is adjusted. If the load increment is appropriate and convergence is likely, ABAQUS continues with the iteration process. With the combination of what the user assign with respect to increment size and maximum number of iterations and the help from the software determining analysis where convergence is unlikely, excessive and needless CPU-time is avoided (ABAQUS (2008)).

6.2.2 Incremental method - Step Module

ABAQUS uses time as the increment factor. The step sequence in ABAQUS provides a convenient way to capture changes in the loading and boundary conditions of the model. Changes can for example be different parts intersecting with each other, removal or addition of parts and any other changes that might occur during the time period of the analysis. ABAQUS differs between initial step

and analysis steps. In the initial step the boundary condition, fields and interactions that are applicable at the very beginning of the analysis is assigned. It needs to be at least one analysis step, but often there are several. As mentioned, the increment is a time increment that the user decides. The load can therefore be applied over a given time interval, and by using multiple analysis steps it is possible to describe a load pattern accurately.

6.3 Special Feature

When dealing with complex FEA models with several parts and difficult geometries, some special features might be useful to ensure that the model gets represented correctly in the analysis. Some of these features will be explained in the following.

6.3.1 Interaction

ABAQUS does not recognize mechanical contact between part instances or regions of an assembly unless contact is specified. Because of this, the analyst need to assign contact properties between surfaces when performing an analysis.

Surface Contact
ABAQUS can handle several different interaction problems, and surface contact is one of them. For surface contact there are two main methods. The first approach is the all-inclusive, where ABAQUS detect every contact pair and determines which face will act as the master and slave surface. This approach can be useful for analyses with few contact pairs. In the second approach, the analyst decides the contact pairs. This approach allows the analyst to determine which of the faces becomes the slave and master surface while determining which surfaces to include in the interaction.

Tie
A tie constraint allows to merge together two regions, although the meshes created on the surfaces of the regions can be different. There will be no relative motion between the parts in a tie constraint. As for a surface contact, tie interactions need a master- and slave surface or node region.

6.3.2 Slave and master surfaces

A contact constraint in a finite element model are applied in a discrete manner. Which means that for a hard contact, a node on one surface is constrained to not penetrate the other surface. For a master-slave contact, nodes on the slave surface cannot penetrate the segments on the master surface. To achieve best possible results of the contact interactions, there are mainly four rules recommended to be followed:

- The slave surface should be meshed finer than the master surface,
- The larger of the two surfaces should act as the master surface,
- If the surfaces are of comparable size, the surface on the stiffer body should act as the master surface,
- The larger of the two surfaces should act as the master surface.

Figure 6.3 shows a penetration of master and slave surfaces. The master surface penetrates into the slave surface due to a coarse discretization. The mesh on these surfaces is therefore not sufficient and should be changed.

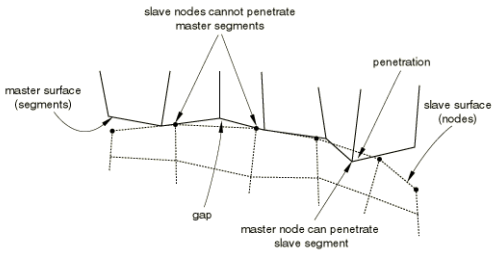

Figure 6.3: Master surface penetrations into the slave surface due to coarse discretization (ABAQUS (2008)).

As described earlier, ABAQUS uses Newton-Rapshon iteration. At the start of each increment and following interaction, ABAQUS checks the state of all the contact interactions. ABAQUS is able to detect changes in the contact interaction at the slave nodes in the updated configurations. If the software detect that a contact node has changed from open to closed or vice versa, ABAQUS mark the changes as *severe discontinuity iterations*. ABAQUS continues to iterate until the equilibrium criterion is satisfied and the discontinuities are approved as small enough.

6.3.3 Kinematic coupling

In a kinematic coupling, a group of slave nodes is constrained to the coupling of translation and rotation of a master node in a customized manner. The user decides what degrees of freedom the slave node that should participate in the constraint should have. Every slave node has a separate relationship to the master node, and the kinematic coupling constraint can be considered as the combination of general master-slave constraints. To be able to implement constraints for multi-point constraints, an additional node is created internally for each slave node. This additional internal node corresponds with the motion of the slave node relative to that of a fully constrained slave node as follows:

Assume that $\mathbf{X}^m$ is the position of the master node and $\mathbf{X}^s$ is the position of the slave node in the reference configuration. The position of the slave node with respect with the master node by assuming the reference configuration position is then:

$$N = \mathbf{X}^s - \mathbf{X}^m \tag{6.6}$$

At the current configuration with $\hat{x}^s$ as the fully constrained slave node position the equation becomes:

$$\hat{x}^s = x^m + n \tag{6.7}$$

n can be written as $n = C(\phi^m) \cdot N$ with $C(\phi^m)$ as the rotation matrix corresponding with the master node rotation, ϕ^m.
The constrained slave node position, which can be selected, can be described as:

$$x^s = \hat{x}^s + y_i e_i \tag{6.8}$$

where e_i works as the current configuration base vectors and y_i are the translation degree of freedom at the additional node. The current base vectors, e_i, rotate from the reference global Cartesian base vectors according to:

$$e_i = C(\phi^m) \cdot e_i \tag{6.9}$$

The slave node translation degree of freedom, *i*, can be described as the release of translation degrees of freedom n the additional node or constraint at $y_i = 0$.

6.4 ABAQUS Analysis Model

The following sections will describe how the analysis model of the wellhead is build in ABAQUS CAE. The model is based on a geometry file provided by prof. Sangesland, Dril-Quip (2019) brochure and recommendations given in ABAQUS user- and theory manuals. There are several ways to use local analysis to detect stress peaks or variation at a given point or area in a global analysis. It is possible to do an analysis studying, for example, displacement, force, stress and curvature. Variation in stress is chosen because it is of interest to discover potential stress concentration factors that the global model is unable to detect.

6.4.1 Geometry

The geometry- and 3D file received from prof. Sangesland could not be directly imported to ABAQUS. It was however possible to read of dimensions from it. Every part is therefore modeled separately based on the file. The revolved modeling technique is used for every part. First, a sketch of the vertical cross section is made. Then, the revolving technique is used to determine which point the cross section should revolve around and the number of degrees. Naturally, a 360 degrees revolve of the cross-section will make a closed loop such as a pipe, while a 180 degree revolve will create only a half pipe. There are several advantages by using 180 degrees and not creating a closed loop with 360 degrees. For example, it is possible to investigate stress and reactions between parts easier, and the required mesh is lowered to only half compared to a full model.

Figure 6.4 shows the given geometry file of the wellhead. Appendix A shows one page of the Dril-Quip brochure, and names of the different components in Figure 6.4 are the same as in the brochure. It should be mentioned that not every component is modelled. There are several reasons why some are left out, but the main reason is that there is information that the manufactures want to keep for themselves. Hence, dimensions and other properties cannot be determined. To speculate on dimensions and properties etc. will only make the results less reliable. It is also possible to obtain accurate results without including all parts in an analysis. It would be very time-consuming to model and run the analysis if all parts were included.

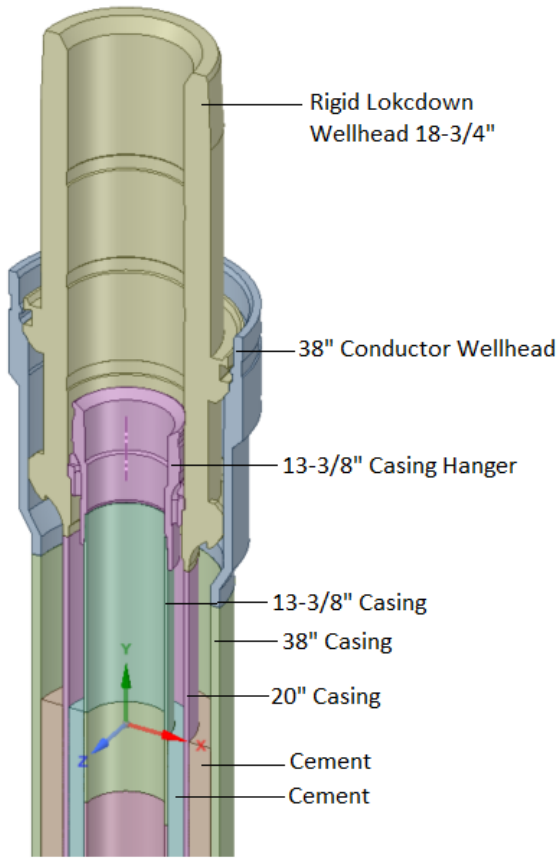

Figure 6.4: Overview of components and assembly in ABAQUS CAE model.

6.4.2 Assembly

After creating the various parts, they need to be assembled in an assembly with position constraints. The model contains only one assembly, and this assembly is created by the different parts of the model. The whole assembly can be seen in Figure 6.4. First a master part is added in the assembly module. Then the other parts, slave parts, are added and constrained relatively to the master part. By using appropriate constraints on the slave parts with respect to the master, it is possible to attach the components at the correct position. Parallel face, face to face and coincide-point constraints have been used to constrain the parts together.

6.4.3 Part - properties

The parts in the assembly needs to be assigned properties. These properties can for instance be materials and profiles for a beam section. The material definition specifies required behaviour of a material and provides the data to that behaviour. It is possible to define different material property to different parts in ABAQUS CAE, and in this analysis a total of two types are used. Properties for steel are used in the wellhead and casings, while properties for cement are used between the casings. Accurate information on the material is difficult to find for both steel and cement. It is assumed that every part made out of steel has the same properties, and the same cement is used during the whole drilling phase. This is most likely not the case, and casings and the wellhead will probably have different steel materials. However, they are assumed to be the same, and the properties for the materials can be seen in Table 6.5.

	Cement	Steel	Unit
Denisty	1400	7850	$[Kg/m^3]$
Poisson's ratio	0.2	0.3	[-]
E-module	20	210	*[GPa]*

Figure 6.5: Material properties for steel and cement used in the analysis.

6.4.4 Mesh

The mesh module allows to generate meshes on assemblies created within ABAQUS/CAE. There are various levels of automation and control options to ensure that the mesh is sufficient for the analysis. As described in Section 6.1, ABAQUS has numerous different types of elements. The quadratic 20-node quadrilateral element with reduced integration, C3D20R, is used for every part in the assembly. Although it might be tempting to use a different type of element than the quadratic C3D20R when modeling a complex geometry, one should be cautious about mixing elements. The quadratic 20-node quadrilateral element with reduced integration, C3D20R, is recommended to use as element type for general analysis without large strains or complex changes in contact conditions. It also performs well for isochoric material behavior and in bending, and rarely exhibits hourglassing despite the reduced integration.

Elements such as triangles and tetrahedals are way easier to use than the C3D20R element when dealing with complex shapes and geometries. However, triangles and tetrahedral elements should be avoided as much as possible in stress analysis problems. The elements are in general overly stiff and exhibit slow convergence

with mesh refinement. This is especially a problem with first-order tetrahedral elements. If it is necessary to use these types of elements, an extremely fine mesh may be required to obtain results of sufficient accuracy. The same problem applies to linear elements, they need a very fine mesh to handle stress accurately. Having a mesh size at these levels are costly in terms of computational time. One method to reduced the overall computational time while maintaining a fine enough mesh is to refine the mesh at areas of interest and locations where stress concentrations are likely to occur. The mesh size will be coarser at the areas with less interest to reduce the computational time.

ABAQUS uses so-called seeds to specify the target mesh density in a region. Seeds can be distributed uniformly along an edge, and it is therefore possible to determine the mesh size along the edge. If more control over the mesh is necessary, the partition tool can be useful to split regions and provide seeds along the created edges. This makes it easier to apply different mesh sizes at different regions of the part. Figure 6.6(a) shows the wellhead sliced and partitioned, while Figure 6.6(b) shows the mesh of the wellhead where different seed numbers have been used in different areas.

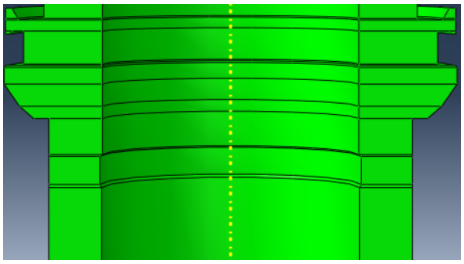

(a) Wellhead sliced and partitioned.

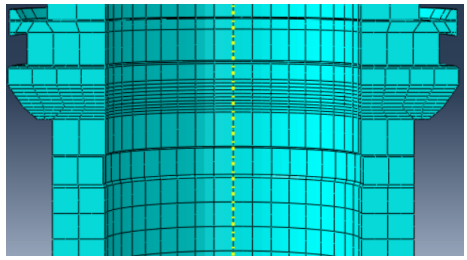

(b) Different mesh at different ares due to different seed numbers.

Figure 6.6: Wellhead sliced and partitioned.

6.4.5 Interactions

In the interaction module, the physical behaviour between parts in the model can be determined and described. This can be interactions between surfaces, fasteners, springs, thermal film conditioning, tie, rigid body to mention some of the possibilities. Constraints defined in the interaction module define constraints on the analysis degrees of freedom, while constraints defined in the assembly module define constraints only to the initial position.

Interaction Constraint

There is a possibility in the interaction module to constrain the degrees of freedom between regions in a model. For example the kinematic coupling constraints, which allows to constrain the motion of a surface to the motion of a single point/node. This is useful when applying concentrated forces and moments, because ABAQUS only applies them at points. When using a kinematic coupling, the force or moment will be distributed to the area that the node is coupled to. In this analysis, the kinematic coupling constraint is used to transfer moment and forces from the riser system. Figure 6.7 shows the kinematic coupling where areas outside of the wellhead are connected to the point at the center of the wellhead.

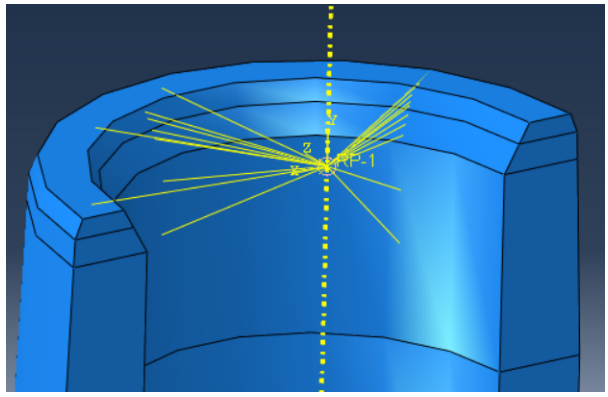

Figure 6.7: Coupling constraint at the wellhead.

Contact

A contact interaction can define tangential behaviour (friction and elastic slip), and normal behaviour (hard or soft). It is necessary to select a master and a slave surface, and the slave surface should have a finer mesh than the master. The contact between steel surfaces are set to have a friction coefficient equal to 0.25. Deciding the exact friction coefficient is difficult, and a value in the intermediate range has been selected (hypertextbook.com (2019)).

6.4.6 Analysis Step

As described i Section 6.2.2, an ABAQUS analysis needs to be built by multiple steps. In the initial step, the boundary- and contact conditions are assigned and will, unless changed, be the same in the next step. In the additional steps, the user can assign realistic load patterns as well as changes in the boundary- and interaction conditions. When performing a large and complex analysis, it is recommended to use a new step at each load, and the loads should be applied in their natural order. Hence, the analyst should be aware of the physical changes during the analysis. The values from the global analysis are applied in only one additional step along the initial step will. The purpose is to obtain the SCF in the wellhead, and the load pattern is assumed to be static and not time depending.

6.4.7 Loads

The wellhead system is mainly subjected to loads from the riser system as described in Chapter 2. The loads that will be applied in the local analysis are taken from the results of the global analyses. In the global analyses, the maximum values are retrieved at the wellhead datum. Hence, forces and moments will be applied at the kinematic coupling as shown in Figure 6.8.

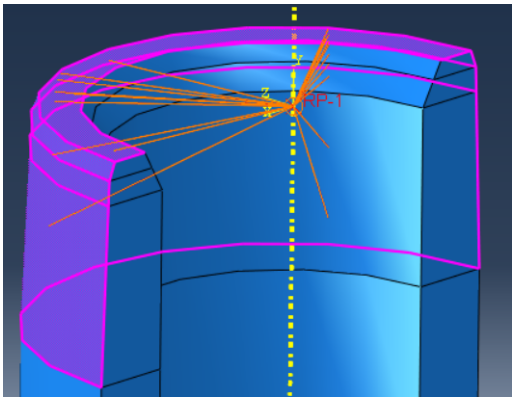

Figure 6.8: Kinematic coupling to apply forces and moments outside of the wellhead at the areas which the BOP connector is fastened.

By applying moment and forces to the kinematic coupling, it should correspond with the super-node called *well_head* in RIFLEX. This is where the fatigue assessments will be calculated. The kinematic coupling area is assumed to be the same as the area that the connector between the wellhead and BOP will cover. The loads acting on the wellhead are three-dimensional and include axial force, shear force and bending force. Since only half of the model is included in the local analysis, only half of the maximal values from the global analysis should be applied. Gravity is implemented in terms of an acceleration of $9.81^{m}/_{s^2}$.

It should be noted that it is the values from the RLWI riser system in RIFLEX that are used in for the local analysis, and not the values for a traditional drilling riser system.

Boundary condition

The assembly of the wellhead system needs to be assigned boundary conditions. There are in total used two different kinds of boundary conditions. For the lower part, the applied boundary condition will be fixed in all degree of freedom that will represent the soil which in the local analysis is assumed to be able to totally constrain the wellhead. At the upper part of the system, the wellhead will have a symmetry boundary condition. ABAQUS has several different options to represent symmetry, and it is often beneficial to model only half or quarter parts to reduce the computational time. Figure 6.9 shows the wellhead with boundary condition where symmetry around the local Y-axis is used. Note the local coordinate system at the bottom left of the figure.

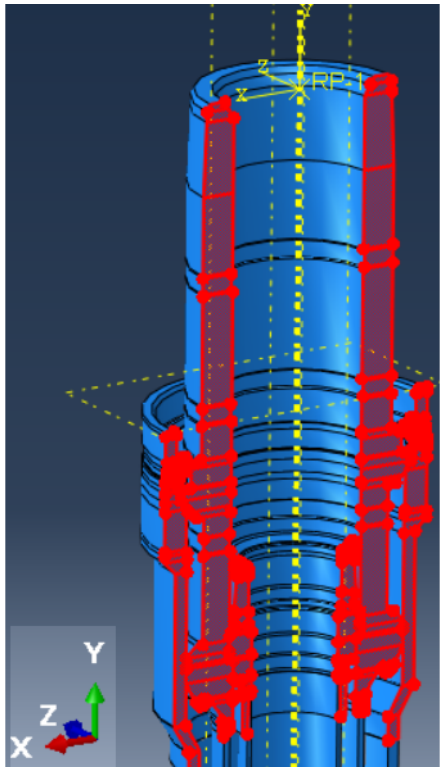

Figure 6.9: Applied boundary conditions at the upper part of the wellhead by using symmetry around axis.

Prepare analysis

Once all the tasks involving defining the model that has been described in this chapter is complete, the job module can be used to analyze the model. After the job is submitted for analysis, ABAQUS/CAE generates an input file representing the model. When performing a lot of similar analysis, it might be useful to only write the input file in ABAQUS/CAE before using an external server with a higher computational capacity to perform the analyses. This opportunity is not used as it does not require many simulations and personal computers nowadays are quite powerful.

Read results - Visualization

The visualization module provides graphical display of finite elements model and results. It contains the model description and result information from the output database. In this case, the maximum values for Von Mises stresses in the wellhead is interesting. Figure 6.10 shows a close-up of the wellhead where the highest stress concentrations occurs.

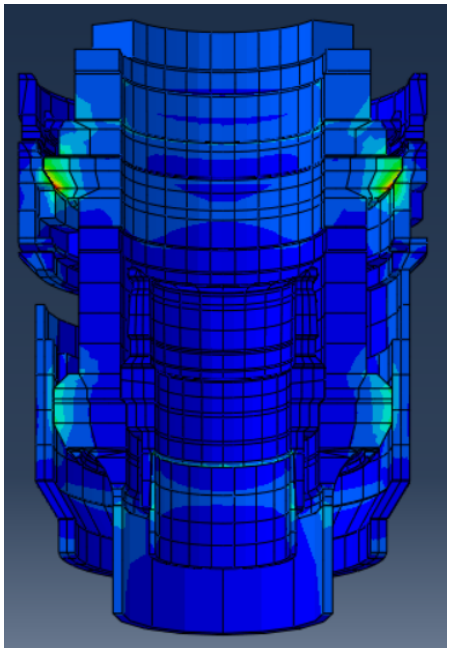

Figure 6.10: Example of stress variation in the wellhead.

6.5 ABAQUS Convergence Study

When performing a FEM analysis, a convergence study of the model should be performed to verify that the mesh is sufficient. One of the main reasons that affects accuracy of an analysis is the mesh density. A too coarse mesh will result in an inaccurate result, too fine mesh will take too long computational time. Hence, using a fine enough mesh to achieve acceptable results while having a mesh that gives a reasonable computational time should be sought. There are in general two ways of mesh refinement, h- and p-refinement. The p-refinement increases the order of the element, while the h-refinement relates to the reduction in the element sizes. The way a h-refinement convergence test is performed is by carrying out several analyses, starting with a coarse mesh and gradually increase the number of elements. It is important when performing such a test that the stresses are retrieved from the same area. The results from the analyses give a graph showing the change in stresses between the mesh sizes. The result should converge towards the correct solution when the number of elements increases.

A convergence study with increasing number of elements(h-refinement) has been conducted for the wellhead model. For analyses with few elements, the same number of seeds has been used everywhere. When the number of elements was increased with a finer mesh and the computational time went up, the edge seed options were used. According to Saint-Venant's Principle, the local stresses in one region do not affect the stresses in another. Therefore, the model can be defined only in particular regions by using partition and seed edges of interest. As shown in Figure 6.6(b), the mesh at the interesting areas is refined while areas with less interest has a coarser mesh.

The test started with an element size equal to 250mm before reducing the size down to 1mm. The convergence test with more detailed values can be found in attachments following the thesis.

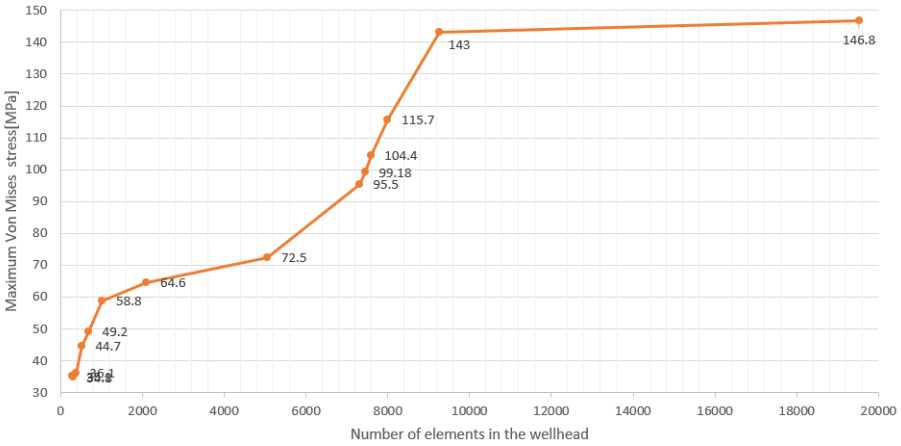

Figure 6.11: Convergence study of wellhead.

The graph shows that the results converge when the element size becomes smaller. Having an increase in maximum stresses when the number of elements is getting higher is as expected. However, the ideally curve is a rapid increase to a maximum value before dropping down and continuing as a straight horizontal line. The difference in stresses between few number and a high number of elements is rather larger. This does not correspond well to the theory about fast convergence for the quadratic C3D20R element. A further investigation and convergence study of the wellhead is recommended. This is not carried out since it is very time consuming, and the goal is to provide an approximately SCF in the wellhead.

It should be noted that there were a singularity at the top of the wellhead. This singularity is located at the interaction area between the BOP connector and the wellhead. This is not considered to be a part of the thesis, and therefore not further discussed.

Chapter 7

Procedures and Simulations

This chapter gives a brief presentation of how the thesis is performed and what types of results that have been achieved. Several software applications have been used, and input data has been transferred between the softwares. Hence, there has been a challenge to correctly transfer data in an appropriate manner.

The first step is to build two models in RIFLEX. A full description of the two models and theory for the software can be found in Chapter 5. The scatter diagram for the Ekofisk field was originally 208 blocks before it was lowered to 58 blocks. The scaled number of blocks reduce the computational time significantly, making it possible to conduct multiple analysis e.g convergence tests in an acceptable manner.

Values for a sea state with significant wave height, $H_S = 2$, and peak period, $Tp = 7$, will be used for convergence studies and to retrieve load values in the global analyses to be used in the local wellhead analysis. A stress concentration factor(SCF) will be calculated by comparing maximum Von Mises stresses between the global- and the local analysis.

For post processing the results and estimate the fatigue damage by the Miner‘s rule, the integrated fatigue filter in RIFLEX will be used. This integrated filter calculates the fatigue damage as described in Chapter 3, including the rainflow counting of load cycles. The SN-curve as described in Section 5.3.12 will be added in the fatigue filter, and the results for the weighted damage of the wellhead will be retrieved. The weighted damage will give the damage for each sea state weighted with the probability of occurrence for each sea state. Both of the riser systems will be analyzed with respect to fatigue damage. Afterwards, the values for the different systems will be compared to each other. According to Reinås

(2012), the planned well production life may be as high as 20-25 years for a well, with an intervention at least every fifth year. With an intervention approximately every fifth year, the number of intervention is set to five in the fatigue assessments.

After the post-processor in RIFLEX is completed, an excel sheets will be created where the results from the fatigue assessments will be calculated. The stress concentration factor from the local analysis are implemented as well as the design fatigue factor(DFF). The excel sheet will compare and add the drilling- and production stage of a well.

7.1 Parameter Studies

To see how the RLWI system behaves compared to the drilling system, two different parameter studies will be performed. The parameter studies can show potential benefits and disadvantages for the two different operations and provide a deeper insight into how they can affect the life of a well.

7.1.1 Currents

There will be no current in the environment affecting the systems for the convergence studies and initial analysis. However, when comparing the fatigue damage for the RLWI- and the drilling system, there will be a total of three different currents that will be studied. The first one, as mentioned, will be without current. The two other currents can be seen in Figure 7.1.

Current (a) has a uniform profile all the way from the sea surface and down to the seafloor with a magnitude of 0.3 m/s. Current (b) has variable speed with zero speed at the seafloor, from the seafloor and up to the surface, the velocity increases and has a maximum speed of 1.2 m/s.

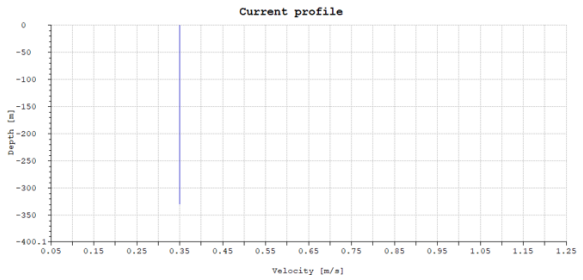

(a) Constant current speed over water depth.

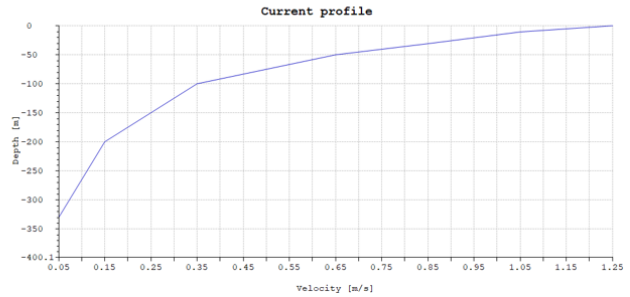

(b) Variable current speed over water depth.

Figure 7.1: The two different currents for the parameter studies.

Current (a) has a uniform profile all the way from the sea surface and down to the seafloor with a magnitude of 0.3 m/s. Current (b) has variable speed with zero speed at the seafloor, from the seafloor and up to the surface, the velocity increases and has a maximum speed of 1.2 m/s.

7.1.2 Top Tension

An advantage of using a lighter system than the traditional system for drilling operation is the reduction of necessary top tension. It is necessary to have sufficient top tension to make sure that the riser system always stays in tension to avoid possible buckling problems. For a heavy system the required top tension will be higher than for a lighter system. Since the RLWI system is much lighter than the drilling system, the top tension will be less.

For the parameter studies, the systems are analyzed with in total three different top tensions. The weight difference between the two risers was estimated at

approximately 1100 kN in Section 5.3.3, and this will be used as difference in top tension between the systems. Table 7.1 gives an overview over the systems and the different top tensions that will be compared to each other.

	RLWI system	Drilling system	Unit
Top tension 1	500	1600	*[kN]*
Top tension 2	600	1700	*[kN]*
Top tension 3	700	1800	*[kN]*

Table 7.1: Overview over top tension variables for the different riser systems.

Chapter 8

Presentation and Evaluation of Results

The main purpose of this thesis is to estimate the fatigue life of a wellhead during the drilling and production stage of a well. It is interesting to investigate the values of accumulated damage from the different types of stages, and also to be able to calculate the fatigue damage for a longer period of time than just the drilling phase. This chapter will include the results and discuss the convergence studies performed in RIFLEX, results from the local analysis of the wellhead and global fatigue analysis for the drilling- and the RLWI system.

8.1 Convergence Study

The same applies to the convergence study in RIFLEX as described in Section 6.5 for the convergence study in ABAQUS. The purpose is to verify the necessary number of elements in order to get reliable results. Too high number of elements will result in unnecessary long computation time, too few elements will give inaccurate results. A value between too few and too many elements is desirable to find a number of elements that provide reasonable computation time and accurate results. A convergence study checking number of elements in the riser- and wellhead section with the RLWI system as basis has been conducted. It is also performed a convergence study to check if the RLWI stack stiffness affects the results. Since the fatigue calculation is for the wellhead, the results has been gathered from this part of the systems. For all the analyses, the sea state has been kept constant. The same applies for other variables such as time period, seed number and currents. As specified in Chapter 7, the environment will have a significant wave height $H_s = 2$, and a peak period, $T_p = 7$. Changing one

variable will ruin the credibility of the results.

For all the convergence studies the maximum bending moment at the wellhead has been compared.

8.1.1 Element Length in the Riser Section

The riser section for the RLWI system consists of only one type of cross section. The upper and lower part of the marine riser will experience larger forces, and it is necessary to have sufficient number of elements to represent these sections properly. However, the riser is divided into equally long element lengths throughout the convergence study and analysis. The results of the convergence study for the number of elements in the riser are given in Figure 8.1.

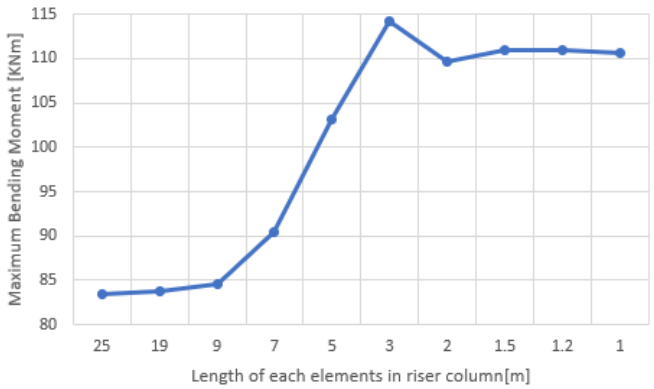

Figure 8.1: Convergence study of RLWI-stack stiffness.

The figure shows the variation between maximum bending moment with the element length as variable. The graph corresponds well to the theory that the graph should rapidly increase with finer mesh before a short decline and a horizontal line. By studying the graph, it appears that the results converge towards approximately *111 KNm*. The value of bending moment with an element length equal to two metres gives *109.6 KNm*. This gives a fault of *1.4 KNm*, which corresponds to an error equal to 1.27%. An error value this low must be considered acceptable for such a complex analysis with so many different parameters. Hence, an element length of two metres is used for the riser for the fatigue analysis.

8.1.2 Element Length in the Wellhead Section

It is of course important to describe the part of the marine riser system where the wellhead is located accurately for a wellhead fatigue analysis. It is therefore conducted a convergence study of the wellhead where the moments acting on the wellhead are located. In RIFLEX, the wellhead datum is located at the end of the well_linetype and at the start of the riser_linetype which is the first segment of the BOP section. Both of the segments closest to the wellhead datum i.e the segment located at the bottom of the BOP and the segment located at the top of the wellhead, are included in this convergence study. The study examine if the number of elements in these two segments affects the maximal moment on the wellhead.

It should be noted that it is expected to have an increase in maximal values with a finer mesh. This area is subjected to large forces, and a fine mesh should be able to detect and describe this better than a coarse mesh.

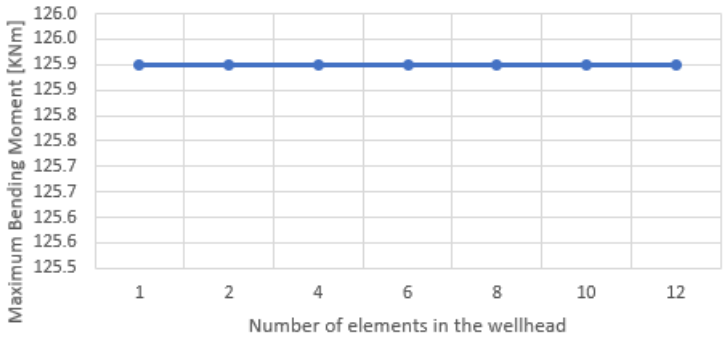

Figure 8.2: Convergence study of number of elements in the wellhead section.

Figure 8.2 shows the results from the convergence study when the number of elements in the top of wellhead area is changed. As seen, the graph is completely horizontal, even with only one element in the segment. This shows that the results converge with only one element in each segment, and there is no need to increase the number of elements in this region as it only will cause additional computational time. This type of convergence graph was not as expected, and a graph looking more like the results from the convergence study of the riser section was predicted. A potential explanation for this result might come from the soil spring in the analysis. The soil spring is the same as in the MARINTEK example, and it might be overly stiff resulting in small lateral deflection and forces at the wellhead datum. Another reason might be the boundary conditions

to the soil-node. All boundary conditions are the same as in the MARINTEK example. The results may be inaccurate if they are not representing the actual problem sufficiently.

8.1.3 Convergence Study of RLWI-stack Stiffness

The properties of the RLWI-stack replacing the LMRP package have been difficult to determine. It is expected that with a softer and more flexible system, the transferred forces from the riser system through the RLWI stack down to the wellhead become smaller. The LMRP package used in the RIFLEX example has properties for bending, axial and torsional stiffness set to 10^{13}. The RLWI stack is smaller and less compact compared to the LMRP-package, and there has been a challenge to determine what stiffness the RLWI stack should have compared to the LMRP-package. Hence, a convergence study with variable stiffness properties for the RLWI-stack has been conducted.

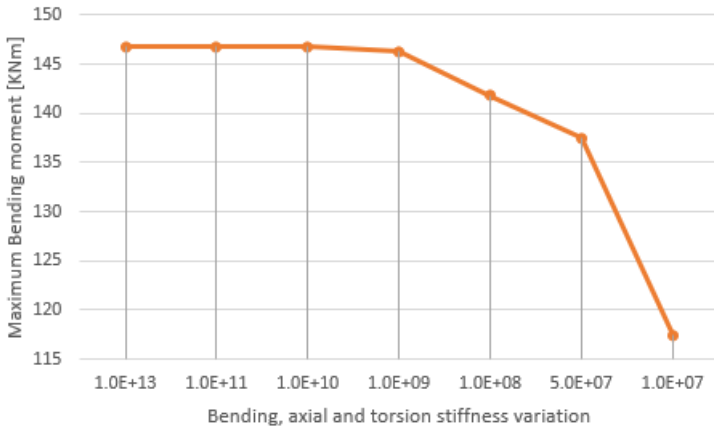

Figure 8.3: Convergence study of RLWI-stack stiffness.

Figure 8.3 shows the results from the convergence study with variable stiffness properties. The graph shows a flat curve for stiffness between 10^{13} to 10^{10} with a small decline at 10^{9}. It was expected to have a decrease in maximum values when the stiffness of RLWI-stack was lowered, and the graph shows the expected. However, this convergence test was conducted early in the thesis, and as desbribed in Section 5.3.6, a value of $^{1}/_{1000}$ of the LMRP stack is used for the RLWI-stack. This will give the same values for maximum bending moment as for the stiff LMRP package. If the RLWI-stack has stiffness, for example, 10^{7}, the fatigue assessments will be a conservative assumption because the transferred forces will be lower with so low stiffness properties.

8.2 Local Analysis of Wellhead

The purpose with the local analysis of the wellhead system is to detect potential stress concentration factors. The wellhead system has some abrupt geometrical changes in geometry, and the wall thickness between the wellhead and the conductor is significant at interfering areas. It is expected that these factors will contribute with stress concentrations at the connection areas between the wellhead and the conductor. Figure 8.4 shows areas with stress concentrations in the wellhead.

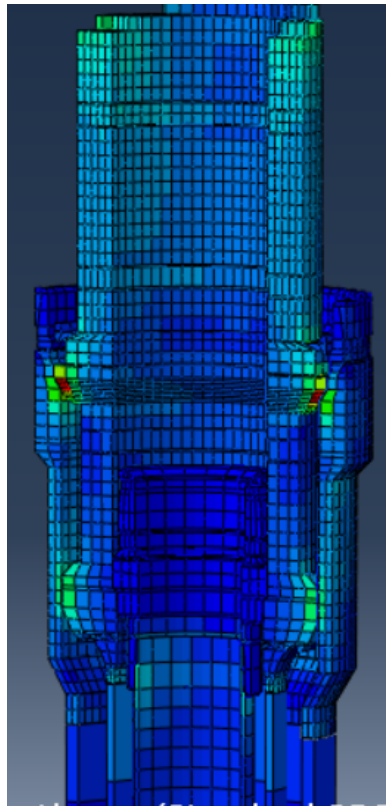

Figure 8.4: Areas with higher stresses in the wellhead system.

8.2.1 Maximum Stress Concentration

The maximum stress concentration measured in the local analysis is located at the 18-3/4” wellhead. This is one of the areas where the wellhead interferes with the conductor. The stress location can be seen in Figure 8.5.

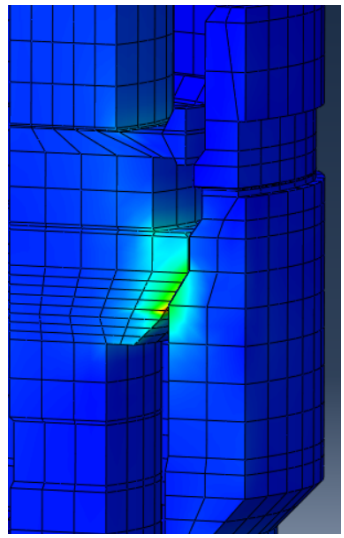

Figure 8.5: SCF in the wellhead in the area between the wellhead and conductor.

It was expected that a stress concentration would be located at the interference between the conductor and wellhead due to the abrupt change in geometry.. There are some other stress concentrations in the wellhead as well, but they are not as high as the one in Figure 8.5. Since it is of interest to find where the maximum SCF is located and where fatigue damage is most likely to occur, the other areas are ignored.

8.2.2 Estimation of SCF

The stress concentration factor is calculated by using the maximum Von Mises stress obtained from the local analysis in ABAQUS and comparing it to the maximum Von Mises stress from RIFLEX. Maximum Von Mises in the local analysis was 146.8 MPa, while for the global analysis in RIFLEX the maximum Von Mises stress was measured to 52.2 MPa. A calculation gives a SCF equal to:

$$SCF = \frac{\Delta\sigma_{maximum}}{\Delta\sigma_{nominal}} \tag{8.1}$$

$$SCF = \frac{146.8MPa}{52.2MPa} \tag{8.2}$$

$$SCF = 2.81 \tag{8.3}$$

A SCF equal to 2.81 is lower than expected. For such a complex system, a SCF in the range between 5-10 can be experienced. The low value of SCF can come from the fact that the local model is simplified, and some of the geometrical challenges in the wellhead system that can cause an increase in SCF may have been omitted. The ABAQUS model is also created with a perfect geometry, so there is no weld or other geometrical imperfections in the analysis. During production of the wellhead this will never be the case, and some kind of imperfections such as welds and holes will always be present. Also. the boundary- and interaction conditions representing the soil and interference between parts can be incorrect resulting in lower stresses.

8.3 Fatigue Assessments

Fatigue assessments for the two different systems have been estimated at the same area in the wellhead. The SN-curve is implemented in the RIFLEX post-processor, while the calculated SCF from the local analysis of the wellhead is implemented afterwards in excel. This is not the best way to implement the SCF, preferably the SCF should be included in the RIFLEX post-processor. As described in Section 3.3.1 for variable amplitude loading, a higher stress amplitude will give a larger damage to the system. When implementing the SCF afterwards many cycles will be calculated in the flatter slope of the SN-curve, while some should actually be in the steeper part of the curve. However, this has proven to be difficult to implement in the RIFLEX post-processor, and the SCF is therefore added as an additional factor as the DFF is.

A failure in the wellhead or conductor will cause a high risk of loss of the well and a potentially blowout with the consequences of human injuries and environmental pollutions. It is also difficult to perform inspections of the wellhead, and according to DNV-C203 (2016), a DFF equal to 10 should be selected for this type of circumstances.

The fatigue life for the two different operations are shown in Figure 8.6(a). The figure shows the lifetime of the well with continuous operations until failure. This will of course not be the case, a drilling and an intervention operation usually last about one month. The drilling phase will have a heavy riser system and a BOP-stack compared to the intervention system with a lighter BOP and RLWI-stack. It is therefore expected that the drilling stage will cause a lot more damage to the wellhead than an intervention operation.

For a well there will only be one drilling phase, but during the life of a well a number of planned or unplanned well interventions may be required. The planned well production life may be as high as 20-25 years, and the need for intervention typically occurs after five years of production. This makes it possible to estimate the damage for a larger lifetime for the well. Figure 8.6(b) shows a comparison between the two operations where it is assumed that the well will need in total five interventions during the lifetime. It is assumed that all interventions will contribute with the same loading on the wellhead.

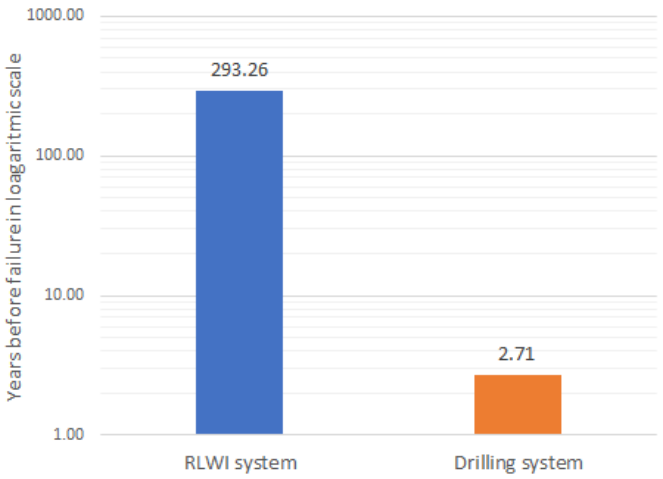

(a) Fatigue life with drilling phase and only one intervention.

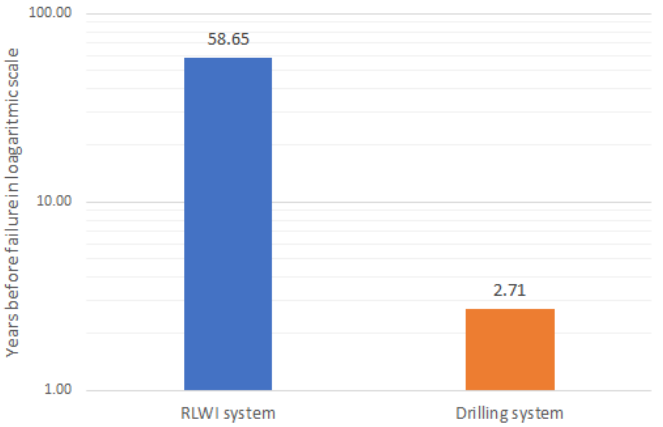

(b) Fatigue life to the well over a lifetime comparing drilling phase and in total five interventions.

Figure 8.6: Fatigue life for the drilling phase with one and five interventions, respectively.

The graph shows that even with five interventions there is a significant difference between the operations and what can be expected of a lifetime. This is as predicted since the drilling phase uses a much heavier equipment and exposes the wellhead for significantly greater forces than an intervention operation.

Figure 8.7 is an extension of Figure 8.6. In this figure, the damage from the drilling phase and the five intervention are added together to estimate the damage over a production period and to evaluate the effects that several interventions have on total damage. The interventions do not contribute much to the total lifetime of the well, even with as many as five interventions, the total damage is not remarkably changed.

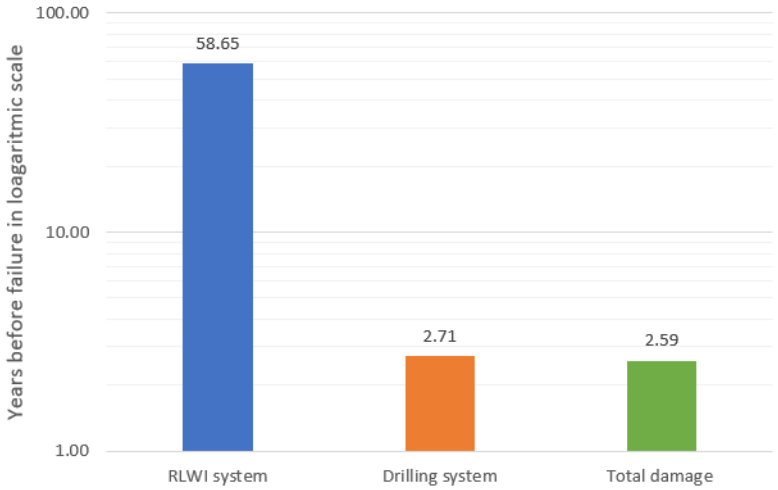

Figure 8.7: Fatigue damage over the lifetime for a well comparing drilling phase and in total five interventions.

Figure 8.8 shows the damage caused by the different systems where fracture occur at a value equal to 1. As already noted, the interventions do not contribute significantly to the total damage. With a total of five interventions these operations account for approximately 4.4% of the total damage. The low values of forces transferred to the wellhead have already been discussed, but the results are perhaps lower than expected considering the amount of interventions.

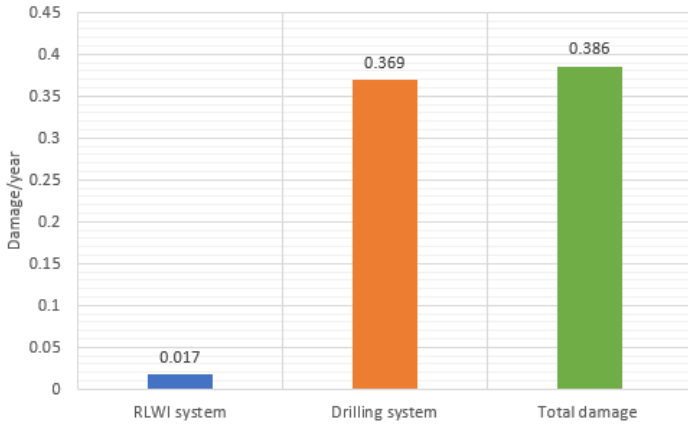

Figure 8.8: Fatigue damage over the lifetime for a well comparing drilling phase with in total five interventions.

8.4 Fatigue Assessments for Parameter Studies

The fatigue assessments for the different parameter studies will be given in the following sub-chapters. These will show and compare how the different systems respond and behave for the different parameters, and a brief discussion will be given for the results. For the studies, the drilling stage will be compared with five interventions that will represent the lifetime of a well before the decommissioning stage. The results that are included are considered to be the most important. Several calculations and graphs showing the fatigue capacity of the well can be found in the attached excel sheets that follows the thesis.

8.4.1 Top Tension

The selected variations in top tension are estimates based on the weight difference of the riser systems described in Chapter 7. The effective tension needs to be positive throughout the riser, otherwise it might buckle. Calculation of the effective tension for the RLWI riser system can be found in Appendix C.

The riser systems can experience in total two different behaviours. The different behaviours are load-dependent which means that the top tension is important. With a high top tension the riser system will become stiffer and will have high axial stresses. If the riser experience a slight deviation, the horizontal component of the axial force will be high and create a large bending moment on the wellhead. The second behaviour can be experienced with a low top tension, then the system will become more flexible. Hence, the riser is more likely to experience relative movements that can cause bending moment on the wellhead.

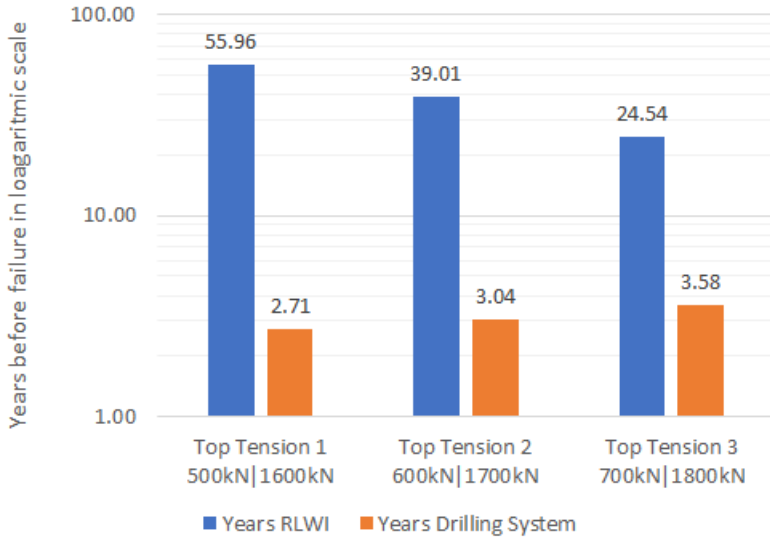

Figure 8.9: Fatigue life for the different systems when using top tension as variable and five interventions.

Figure 8.9 shows the fatigue life for the two different systems with different top tension. The drilling system will have a 32.1% increase in fatigue life using 1800 kN in top tension instead of 1600 kN. The results can be explained by the previously explained behaviour, the riser will become stiffer with an increased top tension. The deviation and the motion of the riser will be less, causing the moment on the wellhead to be reduced. There is no current in the environment in this study, with a significant current a drag force of the riser and vessel could potentially cause a large horizontal force of the system. This could cause and expose the wellhead to greater forces and a reduction in fatigue life.

For the RLWI system, the fatigue life is drastically reduces to only 43.8% of the fatigue life using 700 kN instead of 500 kN as top tension. Hence, Top Tension 1 is closer to maximum fatigue life than both Top Tension 2 and Top Tension 3. It is possible that Top Tension 2 and Top Tension 3 as described above about the potential behaviours, make the system overly stiff. As calculated in Appendix C, the effective tension with a top tension of 500kN is rather high. Values of Top Tension 2 and Top Tension 3 will only give an even higher effective tension in the riser. The riser will become sensitive for deviation leading to a high horizontal component of the axial force. This horizontal component will cause an increase in the bending moment range at the wellhead.

A combination of higher top tension for the drilling phase and a lower top tension for the interventions seems to provide the best solution. This will combine both of the described behaviours, where the RLWI system benefits from a lower top tension giving a more flexible system while the drilling operation benefits from a higher top tension and a more stiff system.

8.4.2 Current

In this parameter study, the effect of current is studied for the systems. The different currents can be seen in Figure 7.1. It is expected that since the drilling riser has larger cross-sections compared with the RLWI system, it will experience a greater effect of currents.

Figure 8.10 shows the results for for the parameter study with varying current levels. Both systems will have a reduced fatigue life when there is no current in the environment. The currents might increase the hydrodynamic damping for the risers. This will cause the excitations to be lowered as well as tge damping will cause the moment range to be reduced. Maximum moment values will however be experienced when the systems are exposed to current, but the moment range is the main reason for fatigue damage. It is therefore expected that a current to a certain level in the environment will increase the fatigue life.

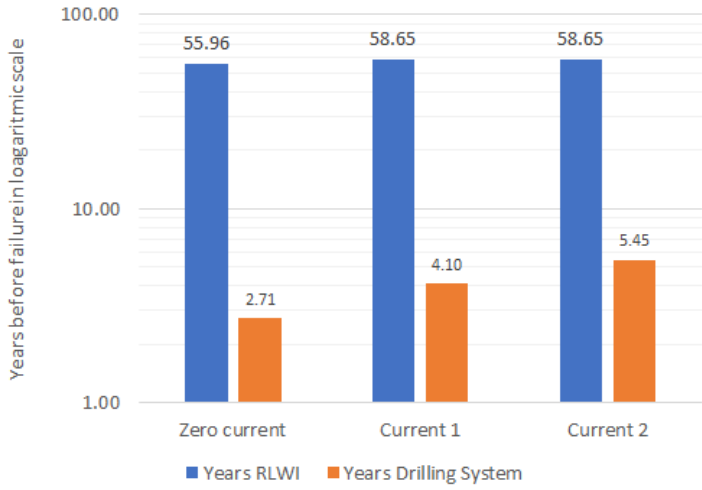

Figure 8.10: Fatigue life for the different systems when using current as parameter study with in total of five interventions.

The results shows the same as it was predicted, the current increases the fatigue life and especially for the drilling system. An explanation to the increased fatigue life may be the hydrodynamic damping contributing more to a riser with greater cross-sections than for a riser with smaller cross-sections. It should be noted that the fatigue life for RLWI system is the same for Current 1 and Current 2 although a similar behaviour as for the drilling riser was expected. Based on the results, it appears that the RLWI riser is not affected of the profile to the currents.

8.5 Discussion

The results from the fatigue assessment in this thesis are highly dependent on the obtained SCF from the local analysis. As already discussed, the SCF were not included in the post-processor in RIFLEX, but added afterwards. The vessel used for the RLWI operation is the same for the drilling operation although this is not the realistic case. This is a limitation factor because the SCF should be included directly in the post processor, and the vessel for a RLWI operation is not the same as for a drilling operation.

8.5.1 Environment

For most offshore operation there will be an operation limit for significant wave height. For a semi submersible as used in the analysis, a typical operation limit is four metres. The scatter diagram has values up to 12 metres, which is probably way higher than the operation limit for both the drilling and intervention operations. The operation limit for the different vessels should have been considered for the fatigue assessments. Hence, the scatter diagram should have been reduced by excluding some of the highest sea states and weighting the reduced scatter diagram so the probability of the sea states would be equal to one. Including higher sea states will give more damage to the system, and the results will therefore be conservative. The conservative scatter diagram will not be a concern for the safety and integrity of the wellhead, but a scatter diagram that includes the operation limit is preferable.

8.5.2 Fatigue Assessments

The results showed that 38.6% of the fatigue life to the wellhead was used during the drilling phase with in total five interventions during the production. It is therefore reasonable to assume that wellhead has sufficient fatigue life to withstand both the drilling- and production stage. The fatigue assessments has proven that an intervention operation contributes with minimal, close to insignificant, damage to the wellhead. Although numbers and types of interventions could vary from well to well and a fatigue assessment for each intervention should be performed, the expected damage should be low. However, after the drilling and production stage, the well should be strong enough to handle the decommissioning. A complete overview of all the three different phases should be investigated to determine if the wellhead is dimensioned appropriately to ensure the integrity of the well.

All fatigue calculations include uncertainties, and small changes in input data can

cause significant changes in the estimated fatigue damage. It is therefore important to evaluate potential uncertainties and verify that the obtained results are accurate and reliable. The SCF has already been discussed several times and remains as the greatest uncertainty. There a more uncertainties than just the SCF, and a list of several other is listed below.

- Environmental conditions and operation limits,
- Use of the same vessel for both kinds of operations,
- Local FE model and SCF,
- Non linear behaviours,
- Properties for RLWI stack and BOP,
- Soil and boundary conditions to the well,
- Temperature variations,
- Number of interventions and type of intervention.

It has been made both a local and global model, which is also an uncertainty. Both models should represent the same case, and how the specification of soil, well and riser system are quite different between the softwares. A confirmation that the local and global analysis represents the same situation should be verified.

Chapter 9

Conclusion

The overall conclusion of this thesis is that the intervention operations compared to the production stage, contributes with minimal, close to insignificant, damage to the wellhead. It seems likely, based on the results, that the wellhead have sufficient fatigue life capacity for both the drilling and production phase with intervention operations. A combination of a higher top tension for the drilling phase and a low top tension for the interventions seems to provide the best solution for fatigue life. This will include two different behaviours where the RLWI system benefits from a lower top tension which provides a more flexible system, while the drilling operation benefits from a higher top tension and a stiffer system. Both systems benefit from a current in the environment, and the results has shown that a larger riser with higher hydrydynamic diameter is more affected than a smaller riser. However, this thesis does not investigate the last phase of the well, and a fatigue damage analysis of the decommissioning phase of the well should be performed to assess whether the well is sufficiently dimensioned or not. Based on the fatigue assessments, it seems likely that the well should be able to withstand the forces from the decommissioning stage.

The thesis is based on a local and global model where the input data for the models has been challenging to acquire, especially data for the RLWI riser system has been challenging. Data for this type of information is often confidential, and some engineering judgment has been necessary to perform the analysis. It is necessary with realistic and relevant data in order to achieve accurate and reliable results. Data and information will vary from situation to situation, and appropriate data is required for a given situation to get results as accurately as possible.

Several convergence studies has been performed to verify and validate the accuracy of the results. Convergence studies for both the local analysis in ABAQUS and global analysis in RIFLEX convergence studies with respect of element size has been performed. The result from the local model gave unexpected results and should therefore be further investigated. For the fatigue calculations in RIFLEX, element sizes providing acceptable accuracy and processing time has been chosen.

9.1 Further work

9.1.1 System

The data and properties for the RLWI system used in this project is only estimates. Hence, values of RLWI-stack should be further investigated to achieve more accurate and reliable results. The semi submersible used for the drilling operation will not be the same for an RLWI operation, and analysis where a vessel used for RLWI operations is included with realistic transfer functions should be performed.

9.1.2 Environment and Loading

RIFLEX is capable to represent loading in three dimensions, while all the wave and current are set as unidirectional in analysis. It is possible that the analysis with loading and currents from different directions can give results that were not taken into account. The water depth is the same for all the analysis, a parameter study for varying water depth should be investigated to determine if it influences the fatigue damage from the drilling and intervention operations. The soil conditions are not taken into account, and a study with a more realistic soil properties should be performed.

9.1.3 Vortex induced vibration

The vortex induced vibration (VIV) has not been a part of this thesis and therefore not further investigated. This is potentially a important parameter for further studies, especially for risers systems with large cross-sections.

Bibliography

ABAQUS, Apr. 2008. *"Getting Started with ABAQUS: Interactive Edition". Dassault Systèmes Simulia Corp., Providence, RI, USA*. Tech. rep.

Almarnaess, A., 1985. Fatigue handbook: offshore steel structures.

Anderson, T. L., 2017. Fracture mechanics: fundamentals and applications. CRC press.

API RP, R., 2016. 17g–recommended practice for completion. Workover Risers,.

API RP 17B, B., 2008. 17b. Recommended practice for flexible pipe 4.

Axtech, ., 2018. *IMR Module Handling Systems*.
URL `http://www.axtech.no/system-solutions/imr-module-handling-systems/`

Bai, Y., Bai, Q., 2005. Subsea pipelines and risers. Elsevier.

Berge, S., 2006. Fatigue and fracture design of marine structures.

Birkeland, S., 2005. Well integrity of subsea wells during light well intervention. Stud. tech. Master Thesis, NTNU.

DNV-C203, Apr. 2016. *Fatigue design of offshore steel structures*. Standard, DNV.

DNV-OS-F201, Oct. 2010. *Dynamic Risers*. Standard, DNV.

DNVGL-RP-0142, Apr. 2015. *wellhead fatigue analysis method*. Standard, DNV.

DNVGL-RP-C203, 2016. Fatigue design of offshore steel structures.

DNVGL-RP-E307, Jul. 2015. *Dynamic positioning systems - operation guidance*. Standard, DNV.

DNVGL-RP-H103, Apr. 2011. *Modelling and Analysis of Marine Operations*. Standard, DNV.

Dril-Quip(2019), Downloaded at 03.05.19 from. *SS Series Subsea Wellhead Systems*.
URL https://www.dril-quip.com/resources/catalogs/04.%20SS%20Series%20Subsea%20Wellhead%20Systems.pdf

Flatern, R. v., 2016. *Upstream Maintenance and Repair*. Intern paper.

Friedberg, R., Joessang, S., Gramstad, B., Dalane, S., et al., 2010. Ss: Subsea well intervention: Experiences from operating new generation riserlesss light well intervention units in the north sea: Challenges and future opportunities. In: Offshore Technology Conference. Offshore Technology Conference.

Harestad, B. ., 2018. *Overflateutstyret til kabeloperasjonen*.
URL https://stier.ndla.no/learningpaths/43/step/414

hypertextbook.com(2019), Downloaded at 02.05.19 from. *Coefficients Of Friction For Steel*.
URL https://hypertextbook.com/facts/2005/steel.shtml

Irvine, T., 2010. Rainflow cycle counting in fatigue analysis. Revision A, Vibrationdata.

Jeddi, D., Palin-Luc, T., 2018. A review about the effects of structural and operational factors on the gigacycle fatigue of steels. Fatigue & Fracture of Engineering Materials & Structures 41 (5), 969–990.

Jensen, ø., 6 2008. Riser less light well intervention (rlwi) - "a success for reducing opex - cost and increasing oil recovery for subsea completed fields". Vol. 4 of 5. StatoilHydro, p. 213, underwater Technology Conference.

Khurana, S., DeWalt, B., Headworth, C., et al., 2003. Well intervention using rigless techniques. In: Offshore Technology Conference. Offshore Technology Conference.

Langen, I., Sigbjörnsson, R., 1979. Dynamisk analyse av konstruksjoner: Dynamic analysis of structures. Tapir.

Larsen, C., 1990. Response modelling of marine risers and pipelines. NTNU, division of Marine Structures.

Lee, Y.-L., Barkey, M. E., Kang, H.-T., 2011. Metal fatigue analysis handbook: practical problem-solving techniques for computer-aided engineering. Elsevier.

Lian, K., 2018. Comparison between a traditional drilling system and riserless light well intervention method considering wellhead fatigue.

Lindland, H. J., Inderberg, O., Braut, A., et al., 2003. New well intervention technology that will enable increase in recovery rate. In: Offshore Technology Conference. Offshore Technology Conference.

Lylund, A., 2015. Analysis of riser-induced loading on wellhead. Master's thesis, NTNU.

Maclachlan, M., 1987. An introduction to marine drilling. Dayton's [Publishing].

Mather, A., 2011. Offshore engineering and production. Edingburgh, UK.: Witherby Publishing Group Ltd.; 3rd ed.

Mathiassen, E., Skeels, H. B., et al., 2008. Field experience with riserless light-well intervention. In: Offshore Technology Conference. Offshore Technology Conference.

Moan, T., 2003. Finite element modelling and analysis of marine structures. Department of Marine Technology, NTNU.

Næss, A. A., Andersson, H., Moan, T., Berge, S., et al., 1985. Fatigue handbook. Tapir, Trondheim.

Paaske, S. ., 2017. *Coiled Tubing*.
URL `https://ndla.no/subjects/subject:6/topic:1:182061/topic:1:178765/resource:1:176779`

Petrowiki(2018), Downloaded at 29.9.18 from:. *Subsea Wellhead System*.
URL `https://petrowiki.org/Subsea_wellhead_systems`

Pettersen, B., 2007. Marin teknikk 3: hydrodynamikk. Dept. of Marin Techn. NTNU, Trondheim, Norway.

Reinås, L., 2012. Wellhead fatigue analysis: Surface casing cement boundary condition for subsea wellhead fatigue analytical models.

Sangesland, S., 2016. *Introduction to drilling and completion of subsea wells*. Unpublished.

Sangesland, S., 2019. E-mail: Specific gravity.

Schlumberger(2018), Downloaded at 29.9.18 from. *Schlumberger glossary:braided line*.
URL https://www.glossary.oilfield.slb.com/en/Terms/b/braided_line.aspx

Sevillano, L. C., De Andrade, J., Stanko, M., Sangesland, S., 2016. Subsea wellhead fatigue analysis with focus on thermal conditions. In: ASME 2016 35th International Conference on Ocean, Offshore and Arctic Engineering. American Society of Mechanical Engineers, pp. V001T01A001–V001T01A001.

Shigley, J., 1989. and mischke, cr. Mechanical Engineering Design, 5th., Ed., Me A+ fie 4a,,+ Graw= Hililnternational 1 (9).

Sintef 1, S., 2017. Riflex 4.10. 1 theory manual.

Sintef 2, S., 2017. Riflex 4.10. 1 user guide. SINTEF Ocean: Trondheim, Norway.

Steinkjer, O., Sodahl, N., Grytoyr, G., 2010. Methodology for time domain fatigue life assessment of risers and umbilicals. In: ASME 2010 29th International Conference on Ocean, Offshore and Arctic Engineering. American Society of Mechanical Engineers, pp. 177–184.

Appendix A

Wellhead model from Dril-Quip brochure

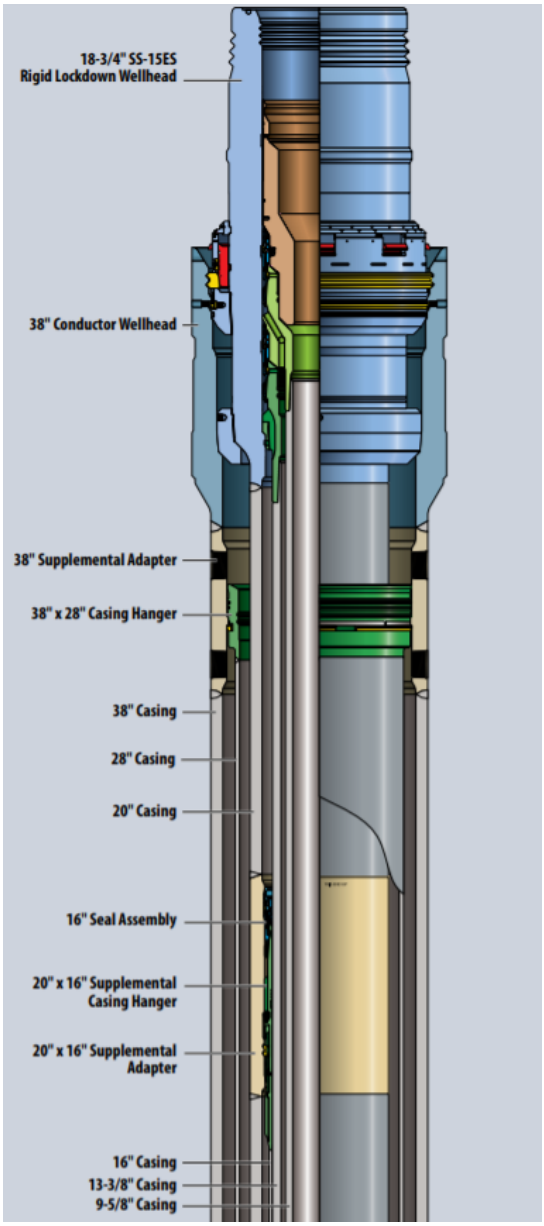

Appendix B

9" RLWI Riser properties

$p := 7850 \frac{kg}{m^3}$ Material density

$E := 2.1 \cdot 10^{11} \frac{N}{m^2}$ Youngs modulus

$v := 0.3$ Poissons ratio

$OD := 228.6mm$ Outer diamer,9"

$t := (25.4)mm$ Wall thickness,1"

$pi := 3.14159$

$G := \frac{E}{2(1 + v)} = 8.077 \times 10^{10} Pa$ Shear modulus

$g = 9.807 \frac{m}{s^2}$ Gravity acceleration

$ID := OD - 2 \cdot t = 177.8 \cdot mm$ Inner diameter

Mass per unit length

$Mperlength := p \cdot \frac{pi}{4}\left(OD^2 - ID^2\right) = 127.285 \frac{kg}{m}$

Axial stiffness: EA

$EA := E \cdot \frac{pi}{4} \cdot \left(OD^2 - ID^2\right) = 3.405 \times 10^9 \cdot N$

Bending Stiffness: EI

$$EI := E \cdot \frac{pi}{64} \cdot \left(OD^4 - ID^4\right) = 1.785 \times 10^7 \cdot N \cdot m^2$$

Torsional Stiffness: TI

$$TI := \frac{E}{2(1 + v)} \cdot \frac{pi \cdot \left(OD^4 - ID^4\right)}{32} = 1.373 \times 10^7 \cdot N \cdot m^2$$

Appendix C

Calculations of Effective tension

$ps := 7850 \frac{kg}{m^3}$ Steel density

$pint := 1600 \frac{kg}{m^3}$ Internal fluid density

$pe := 1025 \frac{kg}{m^3}$ External fluid density

$g = 9.807 \frac{m}{s^2}$ Gravity acceleration

$pi := 3.14159$

$L := 330m$ Water depth

$de := 0.1778m$ External diameter

$di := 0.1524m$ Internal diameter

$Ae := \frac{pi}{4} \cdot de^2 = 0.025\ m^2$ External area

$Ai := \frac{pi}{4} di^2 = 0.018\ m^2$ Internal area

$Atube := Ae - Ai = 6.587 \times 10^{-3}\ m^2$ Pipe wall area

$Wt := ps \cdot Atube \cdot g \cdot L = 167.342 \cdot kN$ Pipe wall weight in air

$Wi := pint \cdot Ai \cdot g \cdot L = 94.453 \cdot kN$ Internal fluid column weight

$We := pe \cdot Ae \cdot g \cdot L = 82.359 \cdot kN$ Displaced fluid weigth

$Waseg := Wt + Wi - We = 179.435kN$ Segment apparent weight

$Pi := pint \cdot g \cdot L = 5.178 \times 10^{3} \cdot kPa$ Internal pressure at bottom

$Pe := pe \cdot g \cdot L = 3.317 \times 10^{3} \cdot kPa$ External pressure at bottom

$Fi := Pi \cdot Ai = 94.453\,kN$ Internal fluid axial force

$Fe := Pe \cdot Ae = 82.359\,kN$ External fluid axial force

$Ttop1 := 1500\,kN$ Top tension 1

$Ttop2 := 1600\,kN$ Top tension 2

$Ttop3 := 1700\,kN$ Top tension 3

$Twt1 := Ttop1 - Wt = 1.333 \times 10^{3} \cdot kN$ True wall tension for Top tension 1

$Twt2 := Ttop2 - Wt = 1.433 \times 10^{3} \cdot kN$ True wall tension for Top tension 2

$Twt3 := Ttop3 - Wt = 1.533 \times 10^{3} \cdot kN$ True wall tension for Top tension 3

$Et1 := Twt1 - Fi + Fe = 1320.6\,kN$ Effective tension with top tension 1

$Et2 := Twt2 - Fi + Fe = 1420.6\,kN$ Effective tension with top tension 2

$Et3 := Twt3 - Fi + Fe = 1520.6\,kN$ Effective tension with top tension 2